Comparison of the Efficacies of Troubleshooting Methodologies for Ventilation Systems – A Field Study.

by

Douglas H. Moody

A thesis submitted in partial fulfillment of the requirements for the degree of

Master of Science

University of Washington

1996

Approved by _____
Chairperson of Supervisory Committee

_____

Program Authorized to Offer Degree Department of Environmental Health

Date 6-3-96

In presenting this thesis in partial fulfillment of the requirements for a Master's Degree at the University of Washington, I agree that the Library shall make its copies freely available for inspection. I further agree that extensive copying of this thesis is allowable only for scholarly purposes, consistent with "fair use" as prescribed in the US Copyright Law. Any other reproduction for any purposes or by any means shall not be allowed without my written permission.

Signature: Douglas H Moody

Date: 6/5/96

University of Washington

Abstract

COMPARISON OF THE EFFICACIES OF TROUBLESHOOTING METHODOLOGIES FOR VENTILATION SYSTEMS – A FIELD STUDY

by Douglas H. Moody

Chairperson of the Supervisory Committee: Associate Professor Steven E. Guffey
Department of Environmental Health

For a ventilation system to control deleterious worker exposures most efficiently, the system ductwork must distribute the airflow in the correct proportions to all the branches serving the hoods. Even if good distribution is established when the system is first installed, the distribution may become increasingly unsatisfactory due to particle settling, alteration from the original design, wear, deformation of the ductwork, and other causes. This means that some hoods may receive excess airflow, while others receive a flow that is inadequate to properly protect workers using the hood. Visual inspection often fails to discover changes to ducts because of their opacity and poor accessibility. Thus, "troubleshooting" must rely on measurements of pressures and flows in the ducts to detect and locate alterations that can affect airflow distribution.

This field study compares the efficacy of six methods of troubleshooting ventilation system branches. Static pressures and airflows were measured on two different systems over a three month period. Repeat measurements were made on each system. The system was then inspected for obstructions or other alterations, cleaned out, and remeasured. Sensitivity and specificity were then calculated for a full range of decision variable thresholds. Methods were compared using receiver operating characteristic curves.

The log transformed static pressure ratio and power loss coefficient (X-value) methods performed much better than the use of hood static pressures alone or the method described in *Industrial Ventilation Manual* (ACGIH, 1995). At a given sensitivity, both methods produce low numbers of costly searches for non-existent alterations. The log transformed static pressure ratio

method does not require a time consuming velocity traverse, and thus may be the method of choice. The common hood static pressure method and the idealized IVM method both performed poorly.

The results of this study provide guidance to industrial hygienists and ventilation professionals as to what troubleshooting methodology is most effective. Equipped with troubleshooting methods that produce few false positives, practitioners may be encouraged to monitor systems more closely and intervene before hood performance has deteriorated to unsatisfactory levels.

TABLE OF CONTENTS

LIST OF FIGURES ii
LIST OF TABLES iv
ABBREVIATIONS AND DEFINITIONS v
CHAPTER 1 – INTRODUCTION 1
Background 2
Description of Troubleshooting Methods 4
Hood Static Pressure Method – One-Sided 4
Industrial Ventilation Method 5
Hood Static Pressure Method – Two-Sided 9
Power Loss Coefficient (X-Value) Method 9
Static Pressure Ratio Method 11
Log Transformed Static Pressure Ratio Method 12
Troubleshooting Test Summary 13
CHAPTER 2 – METHODS 15
Apparatus 16
Ventilation System 16
Equipment 17
Methods 19
Measurement Procedure 19
Analysis Methodology 21
CHAPTER 3 – DISCUSSION OF RESULTS 26
Obstructions 26
ROC Curves 30
ROC Curves for Severe Obstructions 31
ROC Curves for Moderate Alterations 36
ROC Curves for Small Alterations 40
Summary of the Area Under the ROC Curve Results 42
Thresholds and False-Positive Rates 43
Limitations and Research Needs 49
CHAPTER 4 – CONCLUSIONS 51
LIST OF REFERENCES 52
APPENDIX A – CALIBRATION 54
APPENDIX B – EQUATION DERIVATIONS 57
APPENDIX C – EQUIPMENT USED 58
APPENDIX D – BACKGROUND ON ROC CURVES 59
APPENDIX E – LIST OF COMPARISONS 62
APPENDIX F – ORIGINAL DATA 70

LIST OF FIGURES

Number *Page*

Figure 1. Improved Sensitivity of the Log Transformed SP Ratio Method 14
Figure 2. Example of a Severe (Class III) Obstruction 26
Figure 3. Example of a Class I Obstruction (Pieces on the Left), and Class II Obstruction (All Pieces Together) 26
Figure 4. Percent Change in X-values Associated with an Obstruction Class. 29
Figure 5. Percent Change in Log Transformed SP Ratio Associated with an Obstruction Class 29
Figure 6. Obstructions Potentially Misclassified as Class III 30
Figure 7. ROC curve for the One-Sided SPH Method for Class III Obstructions. 32
Figure 8. ROC Curves for the Idealized IVM Method for Class II Obstructions 33
Figure 9. ROC Curves for the Two-Sided SPH Method for Severe Obstructions 34
Figure 10. ROC Curves for the SP Ratio Method for Severe Alterations. 34
Figure 11. ROC Curves for the Log Transformed SP Ratio Method for Severe Obstructions 34
Figure 12. ROC Curves for the X-value Method for Severe Alterations 34
Figure 13. Area Under the ROC Curve Comparisons for Severe Obstructions for Each Random Draw 36
Figure 14. ROC Curves for the Two-Sided SPH Method for Moderate Obstructions 38
Figure 15. ROC Curves for the SP Ratio Method for Moderate Obstructions 38
Figure 16. ROC Curves for the Log Transformed SP Ratio Method for Moderate Obstructions 38
Figure 17. ROC Curves for the X-Value Method for Moderate Obstructions 38
Figure 18. Area Under the Curve Comparisons for Moderate Obstructions for Each Random Draw 39
Figure 19. ROC Curves for the 2-Sided SPH Method for Class I Obstructions 41
Figure 20. ROC Curves for the SP Ratio Method for Class I Obstructions. 41
Figure 21. ROC Curves for Log Transformed SP Ratio Method for Class I Obstructions 41
Figure 22. ROC Curves for the X-value Method for Class I Obstructions. 41
Figure 23. Area Under the Curve Comparisons for Small Obstructions for Each Random Draw. 42
Figure 24. Relationship Between Sensitivity and False Positive Rate as a Function of Threshold for the X-value Method and Class II (Moderate) Obstructions. 44
Figure 25. Relationship Between Sensitivity and False Positive Rate as a Function of Threshold for the Log Transformed SP Ratio Method and Class II (Moderate) Obstructions. 45
Figure 26. Pressure Difference Between Inclined Manometer to the Micromanometer During Calibration on May 1, 1996. 56

Figure 27. Pressure Difference Between the Alnor® Electromanometer and the Inclined Manometer During Calibration. 56
Figure 28. Contingency Table to Calculate the Sensitivity and Specificity of Each Method Given a Specific Decision Threshold 61
Figure 29. Sample Comparison of ROC Curves. The better method has the larger area under the curve and, thus, is higher and to the left in the above diagram. 62

LIST OF TABLES

Number *Page*

Table 1. Summary of Troubleshooting Variables and Rules for a Positive Indication of Alteration 15
Table 2. Time Constant Settings for Pressure Readings 20
Table 3. Description of the Obstruction Classification Codes 21
Table 4. Different determinations of the "truth" based on significance codes 24
Table 5. Contingency Table for Truth Assignment Method B. 24
Table 6. Number and Location of Each Obstruction Class Observed 27
Table 7. Definitions of the Three Levels of ROC Curves Used in this Study 31
Table 8. Summary of the Area Under the Curves for Each Method for Severe (Class III) Obstructions 35
Table 9. Summary of the Area Under the Curves for Each Method for Moderate (Class II) Obstructions 39
Table 10. Summary of the Area Under the Curves for Each Method for Small (Class I) Obstructions 42
Table 11. Thresholds and False-Positive Rates Corresponding to 90% Sensitivity for Each Random Draw by Method and True Obstruction Determination 45
Table 12. Thresholds and False-Positive Rates Corresponding to 80% Sensitivity for Each Random Draw by Method and True Obstruction Determination 47
Table 13. Comparison of Thresholds and False-Positive Rates for the Log Transformed SP Ratio and the X-value Methods for Class II obstructions 47
Table 14. Calibration Data 57

ABBREVIATIONS AND DEFINITIONS

Comparison	A baseline vs. Later measurement pairing from which percent differences are calculated for all methods
df	Density factor: ratio of actual density to standard density
ID	Identification number assigned to a duct
in.w.g.	Inches water guage
Q	Airflow (cubic feet per minute: cfm)
Qact	Actual airflow, takes air density into account (cfm)
ROC curves	Receiver operating characteristic curves
SP	Static pressure (inches water guage: in.w.g.). Represents the difference in pressure between the outside and inside of the duct. Technically it is a negative number, but is frequently referred to as a positive number. In most equations here it is treated as a negative number.
SP ratio	Ratio of the hood to the end static pressures
SPend	Static pressure at the most downstream measurement location of the branch or submain
SPH	Hood static pressure (in.w.g.)
SP:h/j	Ratio of the hood static pressure to that at the downstream junction. (a.k.a.: SP ratio or static pressure ratio)
Threshold(%)	If the percent change in a troubleshooting variable exceeds the "threshold %," the method indicates an obstruction.
TP	Total pressure = SP + VP (in.w.g.)
V	Velocity (feet per minute: fpm)
VP	Velocity pressure

ACKNOWLEDGMENTS

I would like to thank my committee, Dr. Steven Guffey and Dr. Michael Yost, for their valuable support throughout the project and timely response to my many questions. I am gratefully indebted to the many people that assisted with the data collection: Tom Aquino, Derrick Booth, Nancy Simcox, Anne Vielmetti, and Lena Wang. I would especially like to thank David Yu for his assistance throughout the project, but especially when I broke my wrist and could no longer type. Wendall Blum of Blum's Saw in Puyallup, WA was kind enough to allow us unrestricted access to his ventilation systems. I would like to thank Dr. Gerald van Belle for being so giving of his valuable time and statistical expertise. I would like to thank NIOSH for providing funding for myself and this valuable project. I would like to thank Anne Vielmetti for being Anne and keeping me entertained over the long course of this project.

Finally, I would like to thank my parents who made all this possible.

CHAPTER 1 – INTRODUCTION

Proper functioning of an industrial exhaust ventilation system is critical to protecting workers from airborne hazards. Ventilation systems are designed to distribute airflows in appropriate proportions to each work station in an effort to remove hazardous substances. Even if the system provides a good distribution of airflow when it is first installed, alterations (intentional or unintentional) occur over time which tend to redistribute the airflow so that workers at some hoods may not be adequately protected. Particle settling, wear, deformation and denting of the ducts, leaks, and contortion of flex duct are all examples of alterations that may act to redistribute the air. For a system to continue to effectively protect workers, significant changes to the system need to be identified and ameliorated – the process known as "troubleshooting."

Troubleshooting relies on the measurement of flows and pressures because visual inspection alone often fails to identify all changes to the system due the opacity of the ducts and their poor accessibility. Because it is difficult, time consuming, and costly to inspect inside all the ductwork for obstructions, it is important to use a troubleshooting methodology which is highly specific. An effective method would produce few fruitless searches, yet be sensitive to moderate system changes.

Several troubleshooting methodologies are investigated in this study. Two are based on simple measurements of hood static pressures and are probably the most widely used methods. A third method relies on changes to both the hood static pressure and a pressure further downstream. This method is advocated by ACGIH Industrial Ventilation Committee (ACGIH, 1995). Also addressed in this study are three newer methods. Two are based on ratios of static pressures, differing from the ACGIH method by relying solely on measured values and in being quantitative (Guffey, 1994). The last method investigated is dubbed power loss coefficients or "X-values" (Guffey, 1994) and involves a ratio of static and velocity pressures.

The appropriateness of two of the troubleshooting methodologies – static pressure ratios and X-values – have been demonstrated in a laboratory setting (Spann 1993; Colvin 1993). However, before the methods are used widely by practitioners, they should be tested in the relatively uncontrolled conditions of systems currently used in industrial settings. The lab system used in the Spann and Colvin experiments was full-sized, but had only clean, undamaged ducts. Simulating natural "aging" and particle settling would be difficult. In addition, the measurement conditions were nearly ideal and did not address the troubleshooting variables' sensitivity to real world measurement errors.

The purpose of this study is to evaluate these six troubleshooting methodologies under "real world" conditions with respect to their sensitivity in detecting alterations to ventilation systems and their certainty in specifying which ducts have been changed. This is intended to provide guidance for each method on the degree of control that is possible under a regular monitoring and maintenance program. A secondary purpose of the study is to determine what the most appropriate thresholds are for various decision variables employed by each method.

Background

Ventilation systems serve a vital purpose – they protect workers from potentially hazardous exposures. Like people, ventilation systems need to be monitored, evaluated, and maintained to ensure proper functioning.

All too frequently ventilation troubleshooting consists of overly simplistic and qualitative approaches. Waiting for worker complaints or until visible emissions are noted at the hood identifies problems only after exposures have already become severe and already impacted worker health. Worse, if the escaping contaminants are poorly detected by the human senses, exposures could continue indefinitely. Relying on regular visual inspection of the system to identify any changes can permit many system alterations to go unnoticed because they occur within the opaque duct or in areas of poor accessibility.

Many texts discuss troubleshooting ventilation systems, but rely on visual inspection or give little guidance in interpreting changes in performance measures. *Handbook of Ventilation for Contaminant Control* (McDermott, 1995), for example, has one paragraph that addresses troubleshooting:

> Diagnose the problem by thoroughly inspecting the system and by taking pressure and velocity readings .... The visual inspection will reveal closed dampers, open inspection ports, damaged hoods, and ducts, and other common reasons for poor performance. The static pressure measurement at hoods, elbows, and on both sides of air cleaners will show the contribution of each to the overall pressure drop in the system. Static pressure measurements on both sides of the fan show how much pressure the fan is adding. If you know that the system ever operated correctly, try to compare current pressure readings with previous data. If no earlier data are available, try estimating where the pressure drop readings should be from the design tables in Chapter 8 or in the ACGIH *Industrial Ventilation Manual.* For new systems, pressure readings will help detect installation mistakes or blockages due to construction debris.

Notice that no guidance is given as to what percent change in what measures constitutes a substantive change. Without guidance, the reader may choose a low threshold for action, and as a result, waste long periods of time looking in locations where no alterations exist.

What is needed are effective screening tools, like medical screening tests, which indicate the "truth" with relatively little investment. Like medical screening tests, a good troubleshooting method should produce few false negatives. However, it is also important to avoid false positives. A medical screening test which identifies all of those that are diseased is not worthwhile if its false positives results in dangerous and unnecessary surgery. Ventilation troubleshooting is similar. Taking ductwork apart to remove obstructions is often time consuming and expensive. Fruitless searches can consume time, effort, money, and the credibility of the practitioners. A good troubleshooting method identifies where changes likely have occurred, but also reliably rejects cases where no change has occurred. For this study the analysis of troubleshooting methods draws on the use of receiver operating characteristic (ROC) curves developed for the analysis of medical screening tests (see Appendix D) to compare the overall effectiveness of different troubleshooting methods.

Description of Troubleshooting Methods

This section describes the six troubleshooting methods or "screening tools" that are addressed in this study.

Hood Static Pressure Method – One-Sided

The most commonly used troubleshooting methodology in the field and the most frequently described in the ventilation texts is what is called here the "one-sided" hood static pressure method (Alden, 1982; Burton, 1982). Here, the hood static pressure is compared to a previous value. If the hood static pressure has decreased, an obstruction is suspected in the branch or a downstream submain. An increase in SPH is ignored.

There are several shortcomings of this method. First, there are no published and tested guidelines as to what constitutes a significant change in hood static pressure. Second, any change in air resistance at any point in the ventilation system will cause shifts in airflow throughout the system and change the hood static pressures. Thus, hood static pressure values will change even when there are no alterations downstream in the branch due to such things as changes in fan rotation rates and alterations in other ducts. Hood static pressures are sensitive to shifts in airflow, but are very non-specific, leading to a large number of false positives if the Threshold(%) is low. Third, this method may be able to identify only obstructions that occur downstream of the hood measurement location. It is common, however, for obstructions to occur upstream of the SPH location. As mentioned previously, it is frequently necessary to locate the SPH location well downstream of the hood opening because of access and measurement quality issues. This frequently leaves an inaccessible length of duct where obstructions can occur.

In this study, the one-sided hood static pressure method gives a positive indication of alteration if:

$$\% \text{ Change from baseline} > \text{Threshold}(\%) \quad (3)$$

where:

$$\text{Change} = \frac{SPH_{base} - SPH}{SPH_{base}}$$

Industrial Ventilation Method

Probably the most widely published troubleshooting methodology is that described in *Industrial Ventilation* (ACGIH, 1994). It calls for comparisons of observed static pressures to design values. A summary of this procedure follows (changed slightly from original for brevity):

1. Check fan performance against plan, include flow rate, fan static pressure, fan size, inlet and outlet diameters against plan, and the fan speed and direction against design.

2. If fan Inlet static pressure is greater (more negative) than calculated in the design, proceed to Step 3. If fan outlet static pressure is greater (more positive) than design, proceed to Step 7.

3. Measure hood static pressure on each hood and check against design. If correct, go to Step 9; otherwise, continue. Check size and design of hoods and slots against plan, and examine each hood for obstructions [emphasis added].

4. After all hood construction errors and obstructions have been corrected, if hood static pressures are correct, return to Step 1; if too low, proceed to Step 5.

5. Isolate within the duct where the obstruction is located as follows. Measure junction static pressure of the duct and compare with design calculations. If too high at the junction, proceed upstream in the branch until static pressures are too low and isolate the obstruction [emphasis added]. In an area where the loss exceeds design, check the following: angle of junction entries, radii of elbow curvature, duct diameters, and duct obstructions. [Reworded based on personal communication with the section's main author (William Cleary, 1996)]

6. After correcting all construction details which deviate from specifications, return to Step 1.

7. Measure pressure differential across air cleaning device and check against manufacturer's data. If loss is excessive, make necessary corrections and return to Step 1. If loss is less than anticipated, proceed. Check ducts, elbows and entries as in Step 5, and check system discharge type and dimensions against plans.

8. If errors are found, correct and return to Step 1. If no errors can be detected, recheck design against plan, recalculate, and return to Step 1 with new expected design parameters.

9. Measure control velocities at all hoods where possible. If control is inadequate, redesign or modify hood.

10. The above process should be repeated until all defects are corrected and hood static pressures and control velocities are in reasonable agreement with design. The actual hood static pressures should then be recorded for use in periodic system checks.

11. For all of the above measurements, agreement is acceptable if within ±10%.

The IVM procedures cover the fan and air cleaner as well as the duct system. The focus of this study is on steps 1 through 5 as these address the identification of obstructions in the ventilation system branches.

The IVM method assumes that the ventilation system can be accurately characterized using published loss coefficients. However, this is problematic for older systems with dents, leaks, wear, or settling. There is no published data in the literature to support the assumption that loss coefficients correctly model newly installed systems, much less much older systems. There is some evidence that published loss coefficients are unreliable even with relatively new systems. Hoppe (1995) showed that the observed sum of loss coefficients for 87% of the branches of a three year old system deviated from predicted values by more than ±16%. This is not surprising when one considers the variability in the recommended loss coefficients with different sources. For example, up until 1995 IVM recommended using a loss coefficient of 0.27 while ASHRAE Fundamentals (1995) recommended 0.19 for a common elbow geometry (radius/diameter = 2, 5 section). IVM later adopted the ASHRAE values, but ASHRAE soon embraced new values.

In addition, hoods used for a variety of tools do not have published loss coefficients. Without loss coefficients for the elements in a branch, it is not possible to accurately calculate expected losses, static pressures, and flows for the entire system. The IVM method acknowledges this and even states, "It is intended as an initial verification of the design computations and contractor's construction in new systems [commissioning], but it may be used

also for existing systems when design calculations are available or can be recomputed." (ACGIH, 1995). In addition it is common that design data, which is used as the basis for comparison, is frequently lost within a few years of installation.

Step 3 requires that if one hood static pressure differs from expected, then all the hoods need to be inspected to ensure that there are no obstructions and that the hoods are installed as designed. This process has the potential for being excessively time-consuming, especially when inspection involves more than a quick visual check with a flashlight. The hoods of some tools require the hood static pressure measurement to be made well downstream of the hood opening, often with several bends in the duct which prevent inspection by flashlight. An ideal troubleshooting method would not require that all hoods be cleaned out before measurements are made on the ducts, but instead would indicate which of the hoods have undergone some type of change that warrants a visual inspection.

Furthermore, the IVM method provides little guidance as to what changes should be considered significant. It states that, "For all ... measurements, agreement is acceptable within ±10%." However, if the fan rotation rate is set 8% high, then, following the fan laws, total pressure at the fan is going to be 16% high and the total flow rate will be 8% high. In this case, strict interpretation of the IVM method would require all hoods and branches to be inspected for obstructions.

Like the one-sided SPH method, the IVM method identifies only alterations that produce a *decrease* in hood static pressure. Ignoring increased SPH may not be prudent.

Idealized IVM Method

The efficacy of the IVM method depends on both the accuracy of published loss coefficients and the specific use of pressures as indicators. Conceivably, some day practitioners could have perfect knowledge of loss coefficients. However, in analyzing the IVM method, it should not be penalized because current loss coefficients are less than perfectly accurate or, for some components, do not exist. Therefore, we will use the ideal case where the loss coefficients exactly predict the behavior of the original system in every particular way. In other words the

predicted static pressure equals the measured static pressure in a clean system. This modification focuses the analysis on errors due to the method itself. The idealized IVM method is as follows:

1. Measure hood and end static pressures three duct diameters downstream of the hood and three duct diameters upstream of junction, respectively, if feasible. Otherwise, take the best location possible. Record these values as baseline values for later comparison.
2. In future monitoring, if SPH has fallen from its baseline by some threshold percent, SPH-Threshold(%), and SPend has increased by a SPend-Threshold(%), assume that there is an obstruction in the duct. If both of these conditions are not met, assume no change has occurred.

Thus, a positive indication of an obstruction is given by:

$$\text{SPH Change} \geq \text{SPH-Threshold}(\%), \tag{1}$$

and

$$\text{SPend Change} \leq -\ \text{SPend-Threshold}(\%) \tag{2}$$

where:

$$\text{SPH Change} = \frac{SPH_{base} - SPH}{SPH_{base}}, \text{ and}$$

$$\text{SPend Change} = \frac{SP_{end-base} - SP_{end}}{SP_{end-base}}$$

In this study the SPH threshold and the SP_{end} threshold are set to be equal. One might anticipate that even the modified method would still do poorly when there is an obstruction upstream of the hood measurement point and when the resistance to flow has decreased since the last set of measurements (i.e., the branch developed a leak).

Hood Static Pressure Method – Two-Sided

This variation on the one-sided hood static pressure method addresses one problem discussed above – the one-sided SPH method's inability to detect obstructions upstream of the hood measurement point. By investigating increases in hood static pressure as well as decreases (hence, "two-sided"), it should be possible to reduce the number of false negatives and improve sensitivity.

In the two-sided hood static pressure method, a positive indication of change is given by:

$$\text{Change} > \text{Threshold}(\%) \tag{4}$$

Where:

$$\text{Change} = \frac{|SPH_{base} - SPH|}{SPH_{base}}$$

Power Loss Coefficient (X-Value) Method

In troubleshooting ventilation systems, it would be useful to have a value conceptually similar to a resistance which does not change with varying airflow. If an obstruction is in the duct, the "resistance" would increase from baseline. Power loss coefficients, or "X-values", serve this purpose. (Guffey 1994, 1993b; Colvin 1993; Spann, 1993) Changes in X-values from baseline are indicative of changes to the system – larger X-value increases indicate more significant obstructions.

An X-value is a ratio of the lost power (energy dissipated as heat) to the kinetic power at the "exit" point for any continuous portion of the ventilation system. This is represented as:

$$X = \frac{LP}{KP_{exit}} \tag{5}$$

where: LP = loss power
KP_{exit} = kinetic power

This is equivalent to:

$$X = \frac{\left(\sum_i P_{in,i}\right) - P_{exit}}{Q_{exit} VP_{exit}} \qquad (6)$$

where: $P_{in,i}$ = power at upstream boundary "i" = $Q_{in,i}$*$TP_{in,i}$
P_{exit} = power at exit = Q_{exit}*TP_{exit}
Q_{exit} = airflow at exit
VP_{exit} = velocity pressure at exit
TP = Total pressure

X-values can be used to calculate a resistance for any continuous portion of a ventilation system, but for the purposes of this study they are only used on branches. In this case, $\Sigma Q_{in} = Q_{exit}$ and $\Sigma TP_{in} = 0$ (atmospheric pressure), and the X-value for the whole branch up to the "end" measurement point is:

$$X_{end} = \frac{\sum TP_{in,i} - TP_{end}}{VP} = -\frac{TP_{end}}{VP} \qquad (7)$$

Note that the static pressure and total pressure in branches are technically negative values and, thus, need the negative sign for the X-values to be positive. If static pressure is written as a positive values as it is frequently used, this equations reduces down to $X_{end} = \frac{SP_{end} - VP}{VP}$. If baseline X-values have been established, the location of a significant alteration can be determined through a sequential search of the system.

X-values are not truly independent of airflow, but they are stable enough to be useful in troubleshooting (Guffey, 1994). This stability was tested in two laboratory experiments. Spann (1993) demonstrated that X-values varied by less than 2% (C.V.) when air flows varied by up to 50%, a range broader than one might reasonably expect to encounter unless obvious and drastic changes have occurred in the system.

The duct velocities used in these previous laboratory studies were determined by doing three radial Pitot traverses on each duct, resulting in a very accurate estimation of the average air velocity. This was useful to show the effectiveness of each method by minimizing measurement errors. However, most ventilation practitioners are extremely unlikely to do three Pitot traverses for each duct. Therefore, it is necessary to look at the variability of the X-values under field conditions. In this study, VP traverses were done mostly as practitioners would – using a single, ten-point traverse.

In this study, a positive indication of an obstruction by the X-value method is given by:

$$\text{Change for Baseline} \geq \text{Threshold}(\%) \tag{8}$$

Where:

$$\text{Change from Baseline} = \frac{\left|X_{end-base} - X_{end}\right|}{X_{end-base}}$$

$X_{end\text{-}base}$ = baseline X_{end} value

Static Pressure Ratio Method

Calculation of X-values requires time-consuming Pitot traverses to determine velocity pressures. A better method would be one that avoids this, such as the proposed static pressure ratio method. The tradeoff over X-values is that this can only be done on branches; changes to submains cannot be detected with this method as it is used.

It is a fairly straight forward derivation to show that $\frac{X_{hood}+1}{X_{end}+1} = \frac{SPH}{SP_{end}}$ for any branch (see Appendix __). Thus, the static pressure ratio cannot vary unless X_{hood}, X_{end}, or both change. As with X-values, a change in this ratio indicates that a change has occurred somewhere in the branch upstream of the SP_{end} measurement location.

$$SPr\,atio = \frac{SPH}{SP_{end}} \tag{9}$$

where: SPH = hood static pressure
SP_{end} = Static pressure at the end of the branch, upsream of the junction

In this study, a change in SP ratio from baseline indicates a change in the measured duct when

$$\frac{\left|SPratio_{base} - SPratio\right|}{SPratio_{base}} \geq \text{Threshold (\%)} \qquad (10)$$

where: $SPratio_{base}$ = the static pressure ratio at baseline

Log Transformed Static Pressure Ratio Method

The linear static pressure ratio method is not very sensitive when the hood accounts for most of a branch's resistance (i.e., the SP ratio approaches unity). Getting a deviation greater than a 10 percent threshold over a baseline of 0.95 is impossible. For that reason, a method that is more sensitive at the higher static pressure ratios was also analyzed. This was done by taking the log transform of one minus the static pressure ratio and using that as the troubleshooting indicator variable. This is equivalent to making the threshold a moving threshold so that it is smaller at the higher SP ratios; thus, smaller differences can be more significant. This is shown in Equation 11 below.

$$\text{Log transformed SP ratio} = \ln(1 - SPratio) \qquad (11)$$

It is possible for the SP ratio to exceed unity under two conditions: 1) measurement error, and 2) different cross-sectional areas. If SP ratio exceeds unity, Equation 11 has no solution. For that reason, the transformation equation was adjusted as shown in Equation 12. The constant 1.2 is slightly larger than the largest observed static pressure ratio which occurred in a case where the branch duct was smaller in diameter at the hood than it was at the SPend point. This

prevents the value to be logged from ever being negative which would result in an imaginary number. Thus, the log transformed SP ratio variable is given by:

$$\text{Log transformed SP ratio} = \log(1 - \frac{\text{SPr atio}}{1.2}) \qquad (12)$$

As demonstrated in Figure 1, this log transform method is potentially more sensitive when the SP ratio is high. In this case, the hood accounted for most of the pressure loss because it consisted of a 2 inch diameter opening which then expanded to 3 inches. In addition, there was a blockage of 50% of the duct at the 2 inch opening. When this blockage was removed, the system returned to its clean state. At a 5% threshold, the static pressure ratio method did not detect the change as a significant alteration, even though this shift was associated with a 25% change in airflow. The log transformed SP ratio showed a significant 9% change.

Thus, in this study, the log transformed SP ratio test indicates a change when:

$$\frac{\left|\log \text{Trans' dS Pr atio}_{base} - \log \text{Trans' dS Pr atio}\right|}{\log \text{Trans' dS Pr atio}_{base}} \geq \text{Threshold}(\%) \qquad (13)$$

Where: $\text{logTrans'dSPratio}_{base}$ = the baseline log transformed static pressure ratio

Troubleshooting Test Summary

The six methods which were discussed previously are summarized in Table 1 below.

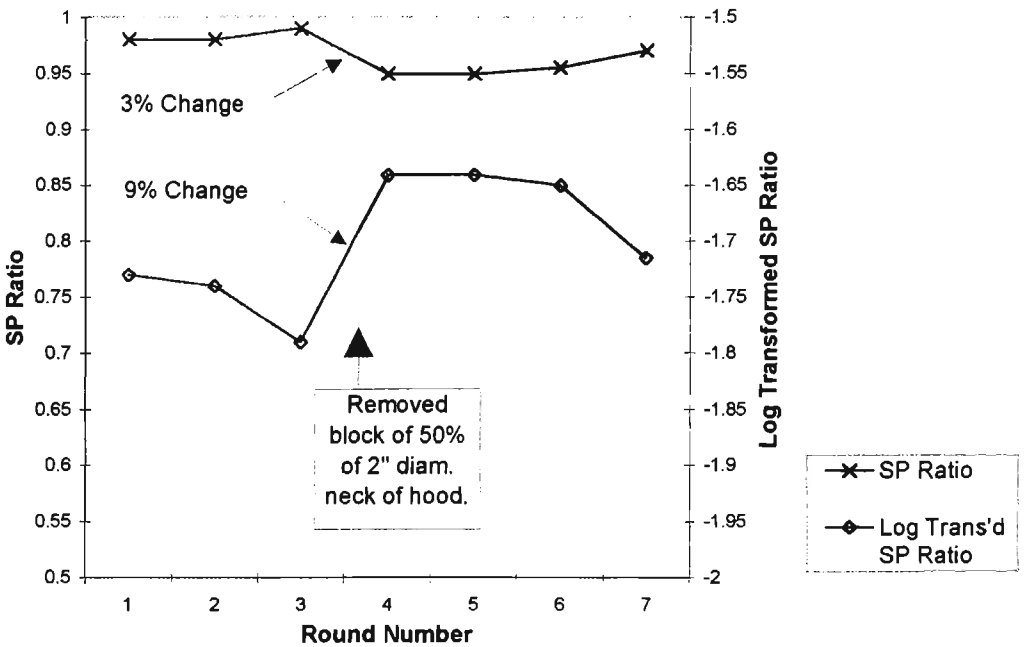

Figure 1. Improved Sensitivity of the Log Transformed SP Ratio Method

Table 1. Summary of Troubleshooting Variables and Rules for a Positive Indication of Alteration

Method	Relative change computed as:	Alteration suspected when:
Idealized IVM	$\frac{SPH_{base} - SPH}{SPH_{base}}$ and $\frac{SP_{end-base} - SP_{end}}{SP_{end-base}}$	SPH Change ≥ SPH Threshold(%) and SP_{end} Change ≤ - SP_{end} Threshold
One-sided SPH	$\frac{SPH_{base} - SPH}{SPH_{base}}$	Change ≥ Threshold(%)
Two-sided SPH	$\frac{\lvert SPH_{base} - SPH \rvert}{SPH_{base}}$	Change ≥ Threshold(%)
X-value	$\frac{\lvert X_{end-base} - X_{end} \rvert}{X_{end-base}}$	Change ≥ Threshold(%)
SP Ratio	$\frac{\lvert SP_{ratio-base} - SP_{ratio} \rvert}{SP_{ratio-base}}$	Change ≥ Threshold(%)
Log Transformed SP Ratio	$\frac{\left\lvert \ln\left(\frac{(1.2 - SP_{ratio-base})}{1.2}\right) - \ln\left(\frac{(1.2 - SP_{ratio})}{1.2}\right) \right\rvert}{\ln\left(\frac{(1.2 - SP_{ratio-base})}{1.2}\right)}$	Change ≥ Threshold(%)

CHAPTER 2 – METHODS

Apparatus

Ventilation System

For the purposes of this study, the ventilation system needed to: 1) be part of an organization that would allow access to the system(s) for the length of the project; 2) be in heavy use such that a variety alterations would likely be observed over the course of the study; 3) have hoods that are not manipulated during the day such that air is redistributed in the system; 4) have conventient measurement locations; and 5) be located close to the University of Washington. Two of the three ventilation systems at Blum Saw in Puyallup, Washington, met all these requirements and served as the focus of the study.

Blum Saw sharpens a variety of metal saw blades for both band saws and circular saws. The two ventilation systems were used to control exposures in metal grinding and brazing operations. One system was dedicated to exposure control with bandsaw grinding – this system was called Bandsaw (or BS). The other system was used for dry operations associated with sharpening of circular saws – this system was called Blum Dry (or BD).

Each system was measured in detail, including duct diameters, length of runs, location and orientation of elbows, and junction angles. Measurement locations for all branches and submains were noted on the drawings. Occasionally, it was necessary to change measurement locations to improve the data quality, in which case these changes were noted on the data files for that day so that they could be taken into account when analyzing the data. A full characterization for each system is included as Appendix A.

In a previous study (Pinsky, 1995), characterization was hampered by changes in the positioning of flexible ducts and adjustible dampers as this alters the airflow and pressures in that branch and throughout the system. However, in these systems none of the branches or

submains used dampers to aid in air distribution. In addition, nearly all of the branches that had flex ducts were firmly set in place, making inadvertent alterations very unlikely. In the cases where flex duct positioning was as issue, pictures were taken for precise repositioning.

Equipment

All pressure measurements were made with the Alnor CompuFlow ElectroManometer, Model 8530D-I (Skokie, IL) with an accuracy of ±1% after zeroing. In the field, the Alnor was frequently rezeroed to insure accurate readings and minimal zero drift.

Static and velocity pressures were taken using Dwyer® stainless steel Pitot tubes (model 167, 1/8 inch diameter, 6 inch insertion depth, 1.5 inch lead tube, Michigan City, IN) which comply with AMCA and ASHRAE specifications (Dwyer Instruments, 1992). Two different tubes were used: one marked for ten-point velocity traverses of 3 inch diameter ducts and the other marked for 4 inch ducts. The duct was divided up into ten equal annular areas, and the traverse points were not positioned in the center of that area, but so that each point represented the mean velocity of that annular area. This log-linear method is considered to be a more accurate traverse method (Ower and Pankhurst, 1977). Each traverse point on the Pitot tubes was scored with a file and marked with indelible ink. During use, static pressure and total pressure holes of the Pitot tube were cleaned when needed. If cleaning was necessary while measuring a branch, all measurements on that branch would be redone. Velocity traverses were done by hand as were all static pressure measurements. The Pitot tubes were connected to the manometer using 1/4 inch ID, 1/16 inch wall thickness Tygon® tubing.

Wet and dry bulb temps were measured using a battery-powered psychrometer (Cole-Parmer Psychro-Dyne) to determine humidity and air density. Temperatures were taken at the start of a sampling day and then repeated when temperature changes were noticed to be potentially significant. Temperatures were assumed to be the same for all hood openings. Note that slight errors in humidity measurements would have very little effect on the air density. Barometric pressures were not taken as they traditionally have minimal effect on the air density.

Calibration

The Alnor® manometer was calibrated against a 4-inch Meriam Wall-Mounted Inclined Manometer (model No. 40HE35WM) and a Dwyer Hook Gage (series 1425, Michigan City, IN) with 0.001 in.w.g. resolution. These three instruments were connected using a valved manifold setup which was then connected to a Meriam hand pump (model B34348). Pressures were set with the hand pump at approximately the following calibration levels (in.w.g.): 0.5, 1, 2, 3, 4.

The Dwyer® hook gage served as the primary standard to which the inclined manometer was calibrated. The inclined manometer was originally calibrated in October of 1994 by Hoppe (1995). The inclined manometer calibration was checked on May 1, 1996. The Alnor® manometer was frequently calibrated to the inclined manometer.

Data Acquisition and Software

To facilitate data collection, the Alnor® manometer was connected to an RS232 Datalogging module (Serial #: 1194, Alnor Instruments, Skokie, IL) which changed the signal from analog to digital so the data could be automatically entered directly into a computer program designed for ventilation measurements (Alnor, 1986). The field computer that was used through February of 1996 was a small, 6.25 × 3.5 × 1 inch Hewlette-Packard 100LX Palmtop PC w/2 MB RAM (Corvallis, OR). In March, the HP 100LX was replaced by a Prolinear MiniNote palmtop computer, Model ME-386 (Prolinear Corp., Arcadia, CA) to increase performance. This direct data logging procedure should have drastically decreased the number of transcription errors that may have occurred in many ventilation studies (Hoppe 1995, Pinsky 1996).

Pressures, wet/dry bulb temperatures, and all comments were input directly into HV_Meas ventilation software developed by Guffey (1996). HV_Meas then calculated air flows, static pressure ratios, and X-values for all branches and submains for which the data was input. HV-Meas also allowed the user to compare pressure and troubleshooting variables to previous values and, thus, check the new data as it is being entered to ensure that the data is entered in the

appropriate cell. Substantial upgrades to this software were made over the course of the study to expand its capabilities, speed, and ease of use. After collection, data from HV_Meas was exported into a spreadsheet program for analysis, organization, and formatting.

Statistical analyses were done using Data Desk, version 5.0 (Data Description, Inc., Ithaca, NY), SPSS (SPSS, Inc., Chicago, IL), and Microsoft Excel, Version 7 (Microsoft Corp., Redmond, WA). Several Excel macros were written to process the data and prepare it for statistical analysis.

Methods

Measurement Procedure

Static pressure measurement locations consisted of 1/8 inch holes. Because the Pitot tube has a rounded right angle to the lead tube, it was necessary to drill an oblong hole for velocity pressure measurements to allow the lead tube to lie flat against the near inside duct wall. All measurement locations were labeled on the duct with indelible ink and covered with tape to prevent airflow leaks.

Measurement positions were chosen pursuant with *Industrial Ventilation* recommendations as much as possible – that is, at least seven duct diameters downstream and two duct diameters upstream of elbows, hoods, expansions, contractions, and other components. This was not always possible because of duct geometry; in these cases, the best available location was chosen. Poor measurement conditions can lead to highly variable and inaccurate data and potentially erroneous conclusions regarding pressures and flows. Because it was frequently difficult to get "ideal" measurement conditions in the field, it was important to look at the variability of each measurement point. Thus, repeat measurement rounds were done so that the impact of the poor measurement locations can be analyzed. For velocity pressures, the measurement location with the least skewed velocity profile was chosen – either SPend, SPmd, or its own location.

For the majority of the static pressure data that was collected, the Alnor® manometer was set with a long time constant (4) to ensure stable readings (see Table 2). Because ten point velocity traverses were done and because it was important to minimize the amount of time it took to do a traverse, a shorter time constant (1) was chosen for velocity pressures. It should be noted that errors in individual measurements tend to balance out over the ten point average.

Table 2. Time Constant Settings for Pressure Readings

Pressure Measurement	Alnor Time Constant Setting	Time to Reach 95% of Input (Seconds)	% Override of Display*
Velocity Pressure	1	5	0
Static Pressure	4	10	100

* The % Override indicates the value that the input must reach to allow the meter to be instantly updated.
Source: Alnor, 1987.

The measurement process required two people to collect the data. To insure consistent positioning of the Pitot tube between different branches and rounds, placement of the tube was always done by the author, while the computer was usually operated by another individual, thoroughly trained in its operation and repeatedly reminded of the readings being taken.

In general, a "round" of pressures was taken starting at the most upstream branch and working from hood static pressure to end static pressure. Sometimes this order was broken to save time in ladder movement and preparation. When one round of measurements for the ventilation system were completed, at least one more round was done to help characterize measurement variability. Because it was necessary to do repeat measurements on the system, each system was done in two parts to allow many repeats on one part of the system. It was assumed that the distribution of the airflow between the two halves of each system was constant over repeated rounds. This was a reasonable assumption because it was difficult for the workers to disrupt airflow during routine work. Even if one hood was changed slightly on the part of the

system that was not being measured, the effect on the other part of the system should have been minimal given that they were separated by large distances.

Once a set of measurement rounds on the system were done, the system was inspected for alterations which may have affected air flow. The inside of the ducts were inspected for clogging, settling, and other alterations with a periscope-like instrument called a borescope (Series 5, Olympus America, Melville, NY). This allowed visual identification of obstructions. The location of each obstruction relative to both geometry and measurement positions was noted on diagrams and in the computer software. In addition, the size of the obstruction and a qualitative estimation of its significance were noted. Later, an obstruction classification code was assigned to each of the noted obstructions (see Table 3).

Table 3. Description of the Obstruction Classification Codes

Obstruction Classification Code	Description
0	No change expected
I	"Modest" obstruction (e.g., clumps that blocked < 20% of the duct area)
II	"Moderate" obstruction (e.g., duct blocked by 20 - 60 %)
III	Severe alteration made (e.g., duct blocked by > 60%)

The branches with obstructions were then cleaned. Before disassembly, the branch sections were marked to ensure that they are returned exactly to their previous positions. Once the system was reassembled, at least one additional round of measurements was taken on the system to see how the obstructions affected the various troubleshooting variables. In addition to incidental obstructions due to the process, obstructions were inserted to increase the number of identified positives.

Analysis Methodology

The first step in the analysis of the data was to double-check that all comments regarding obstructions, measurement changes, and other observations were included in the HV_Meas files

for each round of data collected. A file was prepared which listed each HV_Meas file that was prepared and what was done during the measurement round. For each branch, a drawing was prepared which identified the locations of all measurement points. On the drawing for each branch, a list was kept of all comments for each duct, especially changes in measurement location, when obstructions were identified and removed, and what comparisons were appropriate.

The second step was to determine positive and negative indications from the use of each method on a branch. All positive indications of change for all troubleshooting methodologies in this study were based on a percent change from baseline being greater than some predetermined threshold (see Table 1). Thus, to get a percent change for a troubleshooting variable for a specific branch, it was necessary to have two files to compare, a baseline and an "altered" file. The "altered" branch did not necessarily have an obstruction in it as the alteration occurred elsewhere in the system. Note that the baseline, or "clean," file did not necessarily chronologically precede the altered file during measurement. In fact, it was often the opposite case as described previously – the obstructed system was measured, the alterations were removed, and then the system was then remeasured. The percent change for each troubleshooting variable (SPH, SPend, SP ratio, log transformed SP ratio, and X-values) were calculated for each branch as the percent change from baseline (i.e., $\frac{(\text{base} - \text{altered})}{\text{base}}$).

It was important to ensure that each round of measurement was compared to an appropriate baseline in determining the percent change. It would be incorrect to compare a round of measurement to a baseline that was based on different measurement locations. Similarly, it would be useless to compare a round of measurements to a baseline line if it were not clear if and to what extent the system was altered (i.e., the truth would not be known). In this study, branch comparisons where the alteration status was not known and where the measurement locations had changed between baseline and the altered measurements were omitted from the analysis. The baseline was only changed when information was lacking as to how dirty the system had gotten since baseline. The baseline was then reestablished to represent

new conditions. The matching of baseline and altered branches is shown in detail in Appendix E.

Each comparison between repeat groups (or "conditions") for each duct had a variable number of sets of repeat measurement rounds and, thus, a variable number of possible comparisons. For example, two repeats on the "clean" baseline ("a1" and "a2") and two repeats on the altered system ("b1" and "b2") have four possible comparisons (a1 to b1, a1 to b2, a2 to b1, and a2 to b2). These four possible comparisons are what is referred to as the "repeat group." Consider the case where the entire analysis for a duct consists of one repeat on both the baseline and the altered condition as well as two repeats on both the baseline and the altered condition on another day. If all five points are included in the analysis, there will be four representations of one obstruction and one representation of another obstruction, highly weighting the outcome by how many repeats were done while the first obstruction was in place, rather than equally balanced between all obstructions. To get around this problem, a computer spreadsheet "macro" was written to randomly select one case from each repeat group for each duct. These random draws from the pools of possible comparisons (i.e., repeat groups) were then repeated five times to characterize the range of possible outcomes of the data.

The next step in the analysis was the allocation of each branch "case" to the contingency table. Because the obstructions were of varying sizes it was necessary to define what was considered a "true" obstruction. Three different truth assignment methods were used to test each method's ability to identify severe, moderate, and modest obstructions (see Table 4). Knowing the class of the obstruction allows the proper assignment of the truth. A comparison of the percent change from baseline of the troubleshooting variable to the decision threshold allows the proper assignment of the method indication.

Table 5 shows an example of this contingency table allocation for the X-value method when using truth assignment method B from Table 4 (only considering moderate obstructions). If the X-value changed by more than 10% when a threshold of 10% was employed, the X-value method would have been given a "positive" indication. If a class I (modest) obstruction had

been observed while using truth assignment method B, the X-value method would have scored a "false positive." This contingency table allocation was repeated for all selected branch "cases," allowing the calculation of sensitivity and specificity.

Table 4. Different determinations of the "truth" based on significance codes

Truth assignment method	Duct is considered to have a "true" alteration when:
A	Obstruction class = III (ignoring class II obstructions)
B	Obstruction class = II (ignoring class III obstructions)
C	Obstruction class = I (ignoring class II and III obstructions)

Table 5. Contingency Table for Truth Assignment Method B.

	What was the Obstruction Class? (III=severe, II=moderate, I=modest, 0=none)			
Troubleshooting Method (One-sided or two-sided SPH, IVM, SP ratio, log transformed SP ratio, or X-values)	III	II True obstruction	I	0 No obstruction
Indication of alteration (% Change* ≥ Threshold %)		a†	b	
Indication of NO alteration (% Change* < Threshold %)		c	d	

*For four methods, the % change is technically the absolute value of the % change.

†a, b, c, and d represent the number of occurrences from the data.

To prepare receiver operator characteristic (ROC) curves, a series of contingency tables like that shown in Table 5 were prepared for each method for a range of thresholds from 0% to 100% at 2% intervals. To facilitate this analysis, a computer spreadsheet "macro" was prepared to do these calculations. For the full range of thresholds, sensitivity and false positive rates were plotted to give the ROC curve. See Appendix D for further background on ROC curves. Five random draws from each repeat group of each duct were made to prepare five corresponding ROC curves. The five ROC curves were prepared for each truth assignment method (three) and each troubleshooting method (six) for a total of 90 ROC curves. The area under each ROC curve was then calculated using another spreadsheet macro which employed the trapezoidal method of estimating the area.

In viewing ROC curves, the better method was the one that retains a low false positive rate at a high sensitivity – thus, the ROC curve that was high and to the left. This was the same as saying that that better method had the larger area under the curve. This area has been shown to be mathematically equivalent to the probability that, given two branches, one clean and one obstructed, the troubleshooting method will more likely indicate a "more obstructed" branch in the truly obstructed branch (Beck & Shultz, 1986). By doing random draws on the repeat groups, a pseudo variability of the ROC curves was developed which allowed the determination of which curves had statistically different area under the curves.

CHAPTER 3 – DISCUSSION OF RESULTS

Obstructions

Over the course of the study, a wide variety of obstructions were observed in the ductwork. These included: clogging of metal particulates at sharp bends in the ducts, Stellite saw blade tips; shop rags caught on sheet metal screws; and bent corners of sheet metal within the ductwork leftover from the original installation of the system.

As mentioned in Methods (Chapter 2), an a priori obstruction classification scheme was created (see Table 3). A full list of the obstructions that were associated with all appropriate "baseline-altered" comparisons is presented in Appendix E. Figure 2 is an example of a class III obstruction; the duct was connected directly to the hood and was almost fully blocked with heavy particulate dust and clumps. As Figure 3 shows, not all listed obstructions were "natural." On two separate days, artificial obstructions were inserted to increase the number of true positives for the study. The pieces grouped on the left were categorized as a class I obstruction and all the pieces together as a class II obstruction.

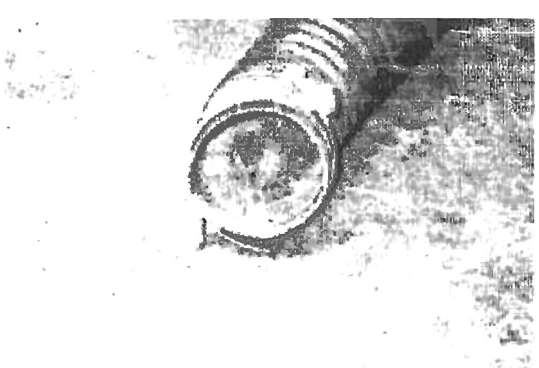

Figure 2. Example of a Severe (Class III) Obstruction

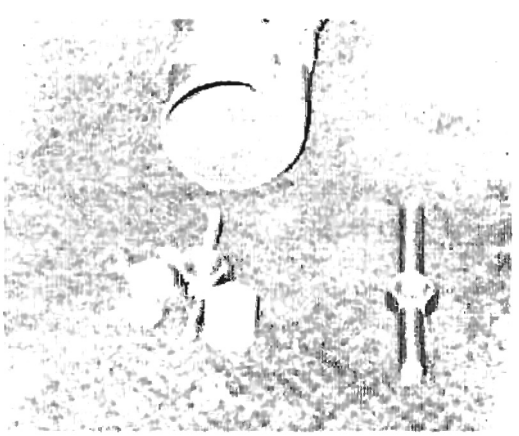

Figure 3. Example of a Class I Obstruction (Pieces on the Left), and Class II Obstruction (All Pieces Together)

Over the three-month course of the study, six class III, seven class II, and thirteen class I obstructions were identified in the two ventilation systems (BS and BD). In addition, there were 47 different cases used in the study where there were no identified obstructions or other alterations. As Table 6 shows, these obstructions were found in a number of different locations – sometimes upstream of the hood static pressure measurement location (SPH) and sometimes, though less frequently, downstream of SPH. The majority of the obstructions were found upstream of the hood measurement location. For each case, there were a variable number of repeat measurements made on both the baseline and altered conditions, yielding a total of 207 possible comparisons.

Table 6. Number and Location of Each Obstruction Class Observed

Obstruction Class	Obstruction Upstream of SPH?	# of Different Cases	Inserted Deliberately
None	--	47	0
I	N	4	2
	Y	9	0
II	N	1	1
	Y	6	1
III	N	2	1
	Y	4	1

The classification of obstructions by severity is subject to human error. This is especially true when the estimated percent of the cross-sectional duct area which is blocked is close to the cutoffs for classification (20% and 60%). Classification relies on visual estimates of obstruction size; however, the accuracy and precision of a visual estimate of the obstruction size is in question. The view through a Borescope may distort the true size of the obstruction. In addition, there are other factors other than the percent of the duct area blocked which influence the effect of the obstruction on the air flow, such as the length of the obstruction, its smoothness, and its orientation and proximity to the elbows. It is important to recognized these

limitations and to understand that misclassifications may occur. These possible misclassifications will affect how well each of the methods are determined to perform, but it is not clear they would affect one method more than another.

The consistency of obstruction classification can be shown by comparing the classification code and the resulting troubleshooting variable values. Troubleshooting variables for class I obstructions should be smaller than class II obstructions, which should in turn be smaller than the most severe obstructions, class III. Figure 4 presents such a graph for X-values. (Note that the large range of values for class III obstructions is not due to unstable X-values, but is instead a result of different obstruction sizes.) It appears that there is significant overlap between class 0, I, and II obstructions, but it also is apparent that there is a general increasing trend. The plot of log transformed SP ratios by obstruction classification shows a similar trend, though with slightly more distinct class II obstructions (see Figure 5). Also shown in this figure are the points on which the two methods disagree (the thresholds were set so that both methods have a 90% sensitivity as shown later in).

A similar figure of log transformed SP ratios versus classification code is presented in Figure 6. It shows a significant amount of overlap between class 0 and I obstructions, but more of a difference between class I and II obstruction, thought there is still some overlap. There seems to be a general trend of increasing change in log transformed SP ratios.

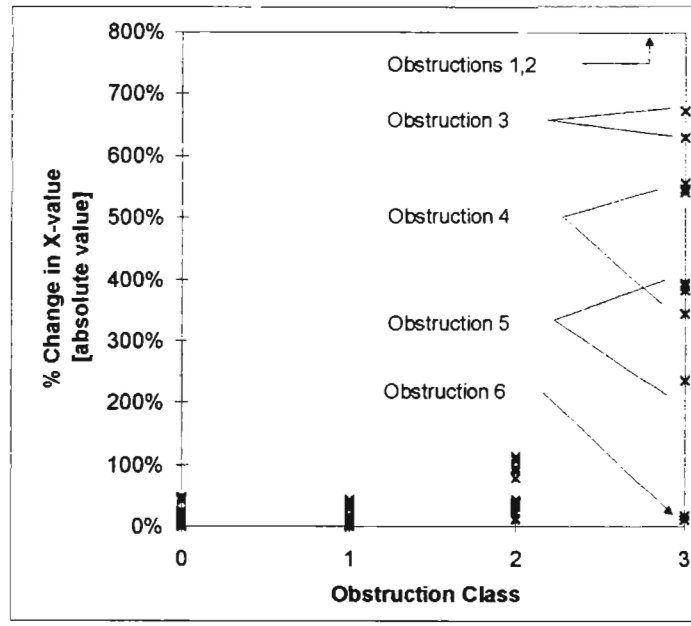

Figure 4. Percent Change in X-values Associated with an Obstruction Class.

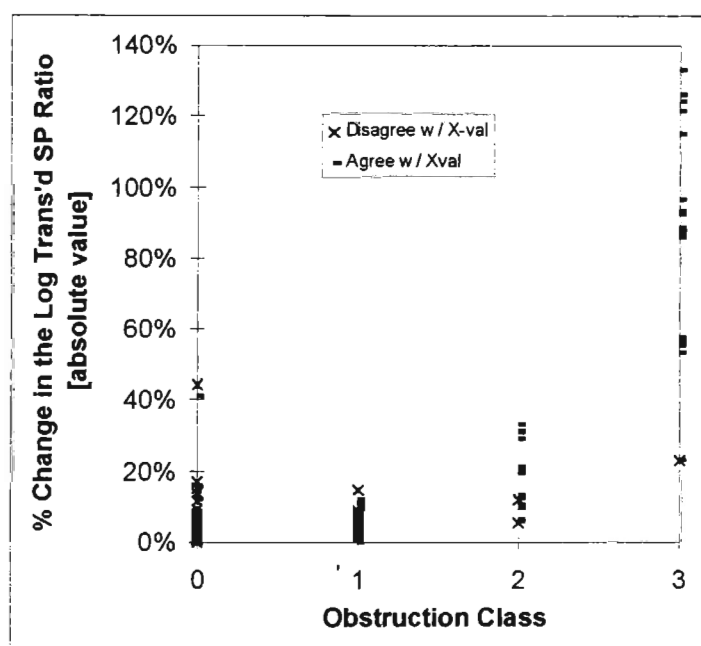

Figure 5. Percent Change in Log Transformed SP Ratio Associated with an Obstruction Class

The severe overlap of one of the class III obstructions with those of class II (Figure 4 and Figure 5) raises the question as to whether this obstruction was misclassified. A review of a photograph that was taken at the time (see Figure 6) revealed that the percent of the duct area that was blocked was overestimated. Taking into account the viewing angle and the depth of the obstruction in the duct, it clear that less than 50% of the duct area was blocked – thus, making it a class II obstruction by definition (see Table 3). The other obstructions that were placed in the duct did not increase the blocked area because they lay on the bottom in front of the machined cone. However, because similar photos were not available to allow a double-check of all obstructions, this obstruction will not be reclassified in the analysis.

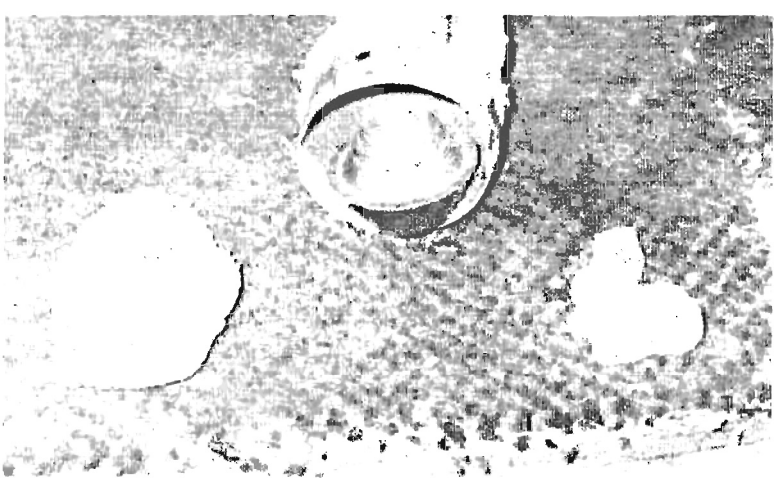

Figure 6. Obstructions Potentially Misclassified as Class III

ROC Curves

Receiver operator characteristic (ROC) curves were prepared as described in Chapter 2 (Methods) and Appendix D. Again, the better method is the one with an ROC curve which is higher and to the left because that corresponds to having more true positives with fewer false positives. The area under the ROC curve is mathematically equivalent to the probability that,

given two branches, one normal and one obstructed, the troubleshooting method will indicate a "more obstructed" branch in the obstructed branch (Beck & Shultz, 1986). An ROC curve was prepared from a random draw from a set of possible comparisons (i.e., baseline-altered pairings). This random draw process was repeated five times for each of the six troubleshooting methods for a total of 30 ROC curves. These 30 ROC curves were repeated three separate times for small (class I), moderate (class II), and severe (class III) obstructions (Table 7).

Table 7. Definitions of the Three Levels of ROC Curves Used in this Study

Truth	Relatioship to Obstruction Class
Severe Obstruction	Class III = true obstruction
	Class II = excluded (1)
	Class 0, I = no obstruction
Moderate Obstruction	Class II = true obstruction
	Class 0, I = no obsruction
	Class III = excluded
Small Obstruction	Class I = true obstruction
	Class 0 = no obstruction
	Class III, II = excluded

(1) Excluded to avoid false positives due to potential misclassification

As will be shown, the one-sided SPH and the idealized IVM methods did poorly even for the most severe obstructions. The log transformed SP ratio method unfailingly out performed the SP ratio method over all obstruction classifications. The X-value and log transformed static pressure ratio methods consistently had similar areas under the curve. The results are presented by obstruction severity.

ROC Curves for Severe Obstructions

For troubleshooting to be useful to ventilation practitioners, it certainly must be able to diagnose severe obstructions (class III). A method that does poorly for gross obstructions is not worthy of further consideration. As will be shown, both the idealized IVM and the one-sided SPH methods did poorly because of their inability to detect obstructions upstream of the SPH measurement location. Thus, they are eliminated from further analysis. The log transformed SP

ratio and "non-log" SP ratio performed nearly perfectly. The X-value method did the next best, followed by the two-sided SPH method.

One-Sided SPH and Idealized IVM

The ROC curves for the one-sided SPH and idealized IVM methods are presented in Figure 7 and Figure 8, respectively. The maximum sensitivity that can be achieved with either the one-sided or idealized IVM methods did not exceed 33% with this data. This is because both methods ignore cases where the SPH increases from its baseline such as when obstructions appear upstream of the hood measurement location. This obstruction location was common at Blum Saw, but may not be for other systems. In fact, only two out of six class III obstructions, or 33%, occurred downstream of the hood static pressure measurement point. These methods performed even worse in identifying moderate and small obstructions (ROC curves not shown).

Because of their poor performance even with the most obvious obstructions, both the one-sided SPH and idealized IVM methods are eliminated from further consideration. The rest of the analysis will focus on the four remaining methods: two-sided SPH, SP ratio, log transformed SP ratio, and X-value.

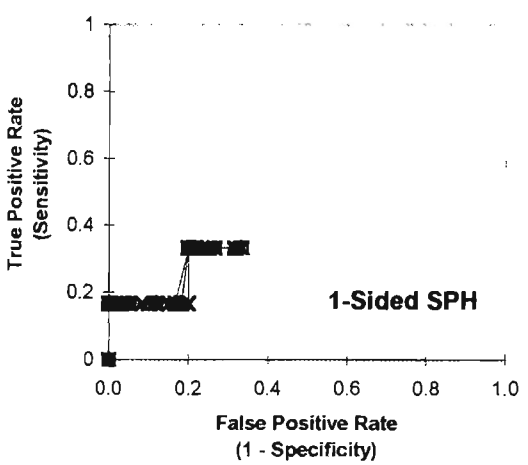

Figure 7. ROC curve for the One-Sided SPH Method for Class III Obstructions.

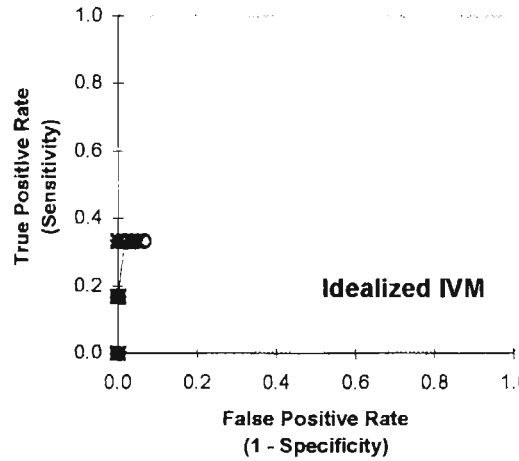

Figure 8. ROC Curves for the Idealized IVM Method for Class II Obstructions

Two-Sided SPH, SP Ratios, and X-value Methods

ROC curves were prepared for the remaining four methods on class III obstructions (class II obstructions were omitted from the analysis because a positive indication of a class II condition is actually a true positive and should not be classified as a false positive). As ROC curves in Figure 9 - Figure 12 show, each of these four methods did reasonably well in determining which branches had been severely altered. The SP ratio (Figure 10) and log transformed SP ratio (Figure 11) did especially well. All methods achieved 100% sensitivity, as expected, for very low thresholds.

It was interesting to note, though, that with all the methods the area under the ROC curve was not unity (perfect performance) as one would hope for severe obstructions. There were some thresholds for each of the methods at which at least one false positive and one false negative occurred – the basic requirement of an imperfect ROC curve. Most of these points, but not all, were associated with the occurrence of obstruction 6 (see Figure 4 and Figure 6).

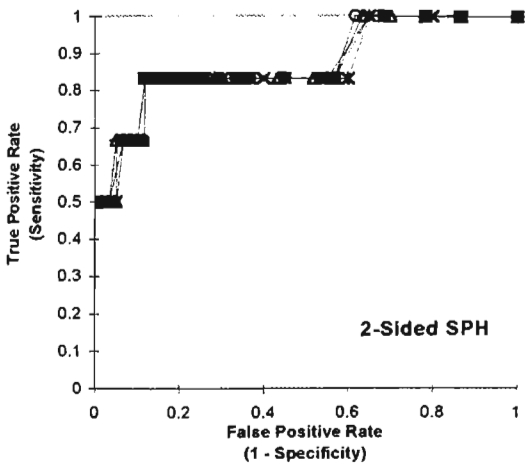

Figure 9. ROC Curves for the Two-Sided SPH Method for Severe Obstructions

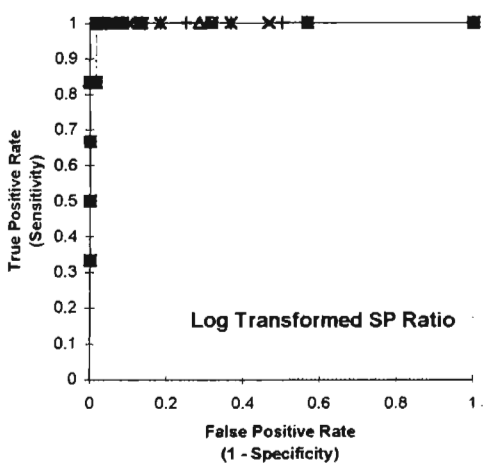

Figure 11. ROC Curves for the Log Transformed SP Ratio Method for Severe Obstructions

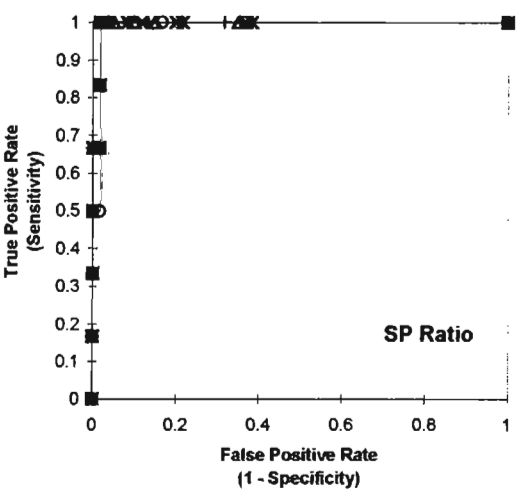

Figure 10. ROC Curves for the SP Ratio Method for Severe Alterations.

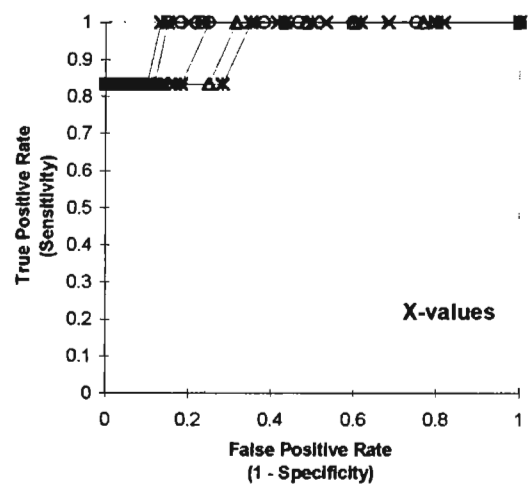

Figure 12. ROC Curves for the X-value Method for Severe Alterations

The areas under the curves for each of the five repeat random draws are summarized in Table 8. Sensitivity and false-positive rate were calculated for each method on the same random draw data. It is clear from the graph of the areas under the curves (Figure 13) that for severe obstructions the four methods' relative performances were consistent. Both methods that rely on ratios of static pressures, the SP ratio method and the log transformed SP ratio method, were almost perfect in identifying the most severe alterations, with the log transformed SP ratio method having a slightly larger area under the curve than the non-transformed approach.

The X-value method was the next best, but had a significantly smaller area under the curve than either of the static pressure ratio approaches. This reduced area under the curve resulted from the occurrence of obstruction6. Also notice that the areas associated with the X-values were much less stable than they were with the other methods. The standard deviation for the X-value method's areas under the curve was over seven times larger than the next closest one. The percent change in the X-values for the various repeats on this percent misclassification varied from 11 to 17% because of a relatively large variation in the average velocity. Thresholds in this range will sometimes indicate a false negative depending on the random draw. This and a difference in false positive rates between 11 and 17% accounts for the larger variability. Because X-values are dependent on accurate velocity determinations and such determinations are very difficult with a single velocity traverse, they tend to be less stable than methods dependent only on static pressures.

Table 8. Summary of the Area Under the Curves for Each Method for Severe (Class III) Obstructions.

	Random Draw #					Mean	St.Dev	Range	
Method	1	2	3	4	5			Min	Max
2-Sided SPH	0.865	0.864	0.865	0.864	0.860	0.864	0.002	0.860	0.865
SP Ratio	0.994	0.994	0.992	0.994	0.994	0.994	0.001	0.992	0.994
Log Trans'd SP Ratio	0.997	0.997	0.997	0.997	0.997	0.997	0.000	0.997	0.997
X-value	0.964	0.953	0.978	0.981	0.947	0.964	0.015	0.947	0.981

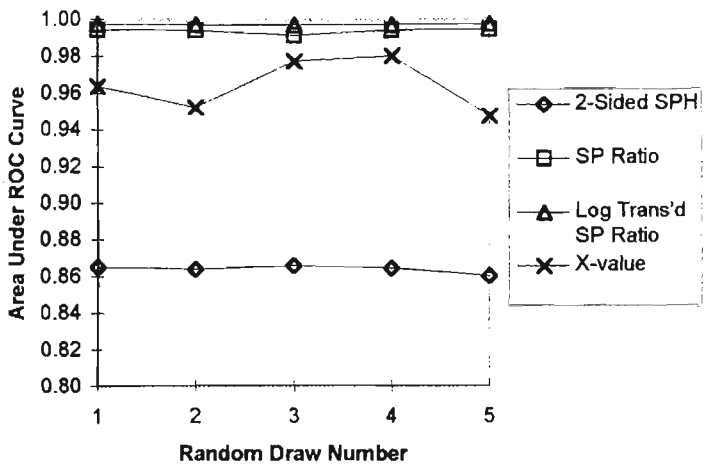

Figure 13. Area Under the ROC Curve Comparisons for Severe Obstructions for Each Random Draw

The worst of the four remaining methods for finding the most severe obstructions was the two-sided hood static pressure method. In Figure 13 and Table 8 the two-sided method had the smallest area under the ROC curve.

As shown in Table 6 the ROC curves on severe obstructions were based on only 6 different obstructions, though several repeats were done on them to yield a total of 24 possible comparisons (the sensitivity is based on six baseline-altered comparisons). If a larger number of serious obstructions had been found, it is possible that the relative performance of the methods would have shifted somewhat. By including less severe class III obstructions, this issue should clarified.

ROC Curves for Moderate Alterations

The most serious obstructions should be discovered with any method. One-sided SPH and idealized IVM methods failed that test. Their results were even worse for less severe obstructions and are dropped from further consideration.

With the remaining four methodologies, the more interesting question is: which method is better at identifying more moderate (class II) obstructions in this study? As will be shown, the X-value method does slightly better than the SP ratio and the log transformed SP ratio method in identifying these moderate obstructions.

Figure 14 - Figure 17 present the ROC curves for all class II obstructions with class III obstructions omitted from the analysis. As expected, ROC curves are less "ideal" than those for the severe obstructions because there were more false positives at a given sensitivity – the ROC curves are less high and to the left.

Table 3 and Figure 18 present the area under the curves for each of the five random repeat draws from the data (class III cases excluded). Again, the two-sided SPH method did not perform as well as the other three methods; its average area under the curve was 0.585 where as those for the other methods were all over 0.90.

The log transformed SP ratio and the X-value methods had the best area-under-the-ROC-curve performance, slightly but consistently higher than the untransformed SP ratio method (Figure 18). When comparing the log transformed SP ratio and the X-value method, the X-value method had the highest areas under the curve in all random draws.

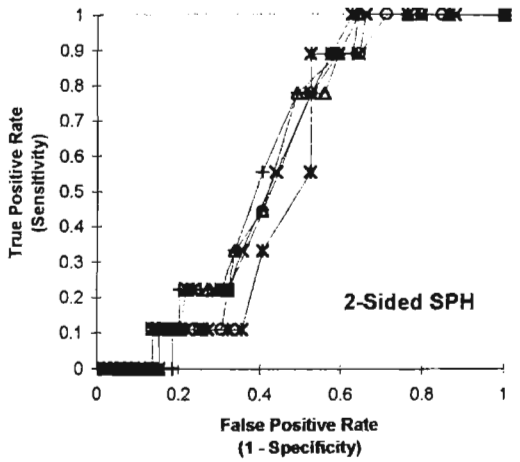

Figure 14. ROC Curves for the Two-Sided SPH Method for Moderate Obstructions

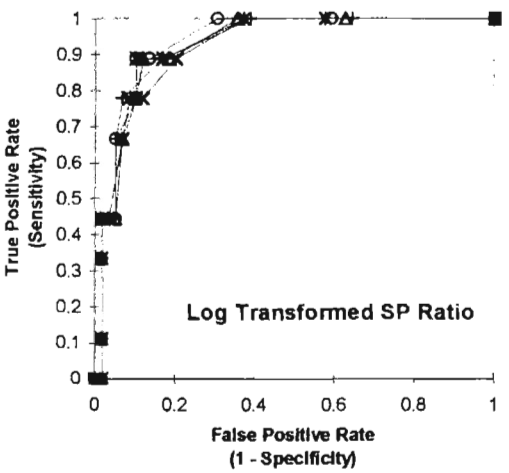

Figure 16. ROC Curves for the Log Transformed SP Ratio Method for Moderate Obstructions

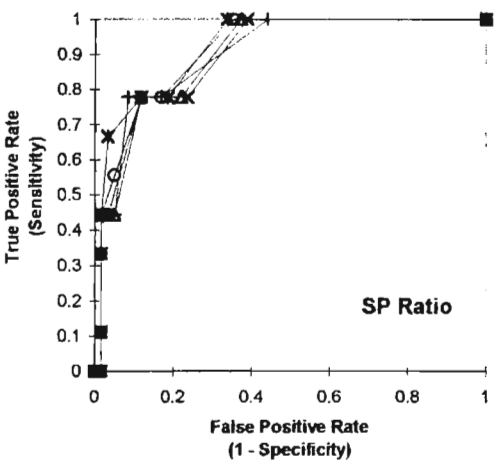

Figure 15. ROC Curves for the SP Ratio Method for Moderate Obstructions

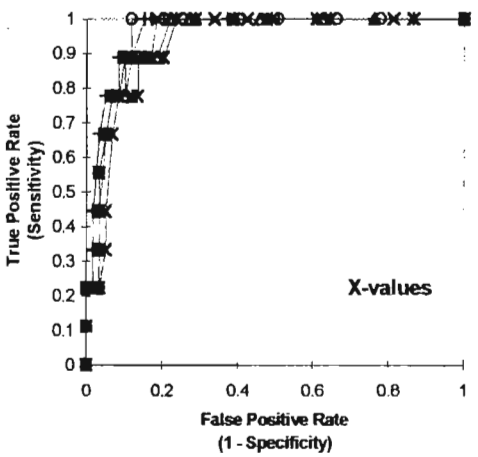

Figure 17. ROC Curves for the X-Value Method for Moderate Obstructions

Table 9. Summary of the Area Under the Curves for Each Method for Moderate (Class II) Obstructions.

	Random Draw #					Mean	St.Dev	Range	
Method	6	7	8	9	10			Min	Max
2-Sided SPH	0.607	0.599	0.577	0.591	0.555	0.586	0.021	0.555	0.607
SP Ratio	0.902	0.898	0.911	0.897	0.920	0.906	0.010	0.897	0.920
Log Trans'd SP Ratio	0.930	0.927	0.937	0.923	0.930	0.930	0.005	0.923	0.937
X-value	0.961	0.942	0.953	0.933	0.943	0.946	0.011	0.933	0.961

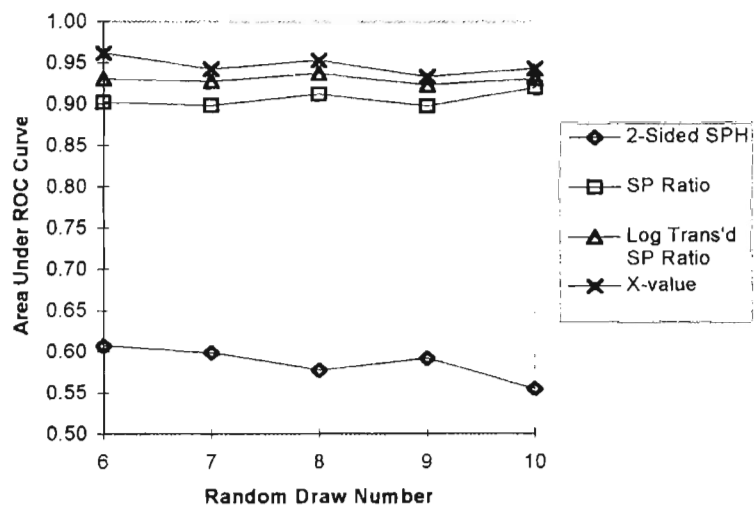

Figure 18. Area Under the Curve Comparisons for Moderate Obstructions for Each Random Draw

Finally, these results for moderate (class II) alterations should be qualified because they are based on only seven different obstructions. On the other hand, the total number of repeat comparisons totaled 18, minimizing the effects of any one measurement error. A larger sample of class II obstructions would strengthen these conclusions, but probably would not change them significantly.

ROC Curves for Small Alterations

The most challenging test of a troubleshooting methodology is how well it can detect small obstructions. This is done by looking at the ROC curves for only class I obstructions (modest changes) and ignoring the class II and III obstructions. Even though there was a significant amount of overlap (Figure 4) between clean and class I obstructions. The X-value method was able to do much better than the other methods at identifying these small obstructions.

Figure 19 - Figure 22, show the ROC curves for this analysis. As expected, there was much more variability in the ROC curves because the small changes in the troubleshooting variables that are associated with these class I obstructions are in the range of measurement variability. The ROC curves for X-values (Figure 22) were particularly variable.

One the other hand, the X-value method demonstrated a consistently higher area under the curve for these modest obstructions (see Table 10 and Figure 23). However, the sensitivity and false-positive rate of the X-value method were much more variable. The standard deviation for the X-value method was 0.063, close to three times that of any of the other methods and six times larger than what was determined for class II obstructions (Table 9). As Figure 23 shows, the method with the next highest area under the curve was the log transformed SP ratio method, followed by the SP ratio method, then the two-sided SPH method. This ranking held for all five random draws from the data.

These findings suggest that one could detect even small obstructions using X-values, especially if the variability of X-values were reduced by improvements in measurement techniques.

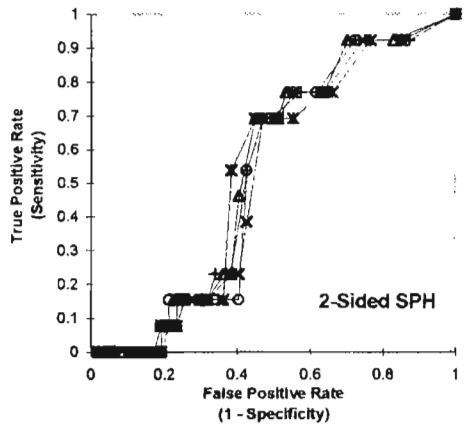

Figure 19. ROC Curves for the 2-Sided SPH Method for Class I Obstructions

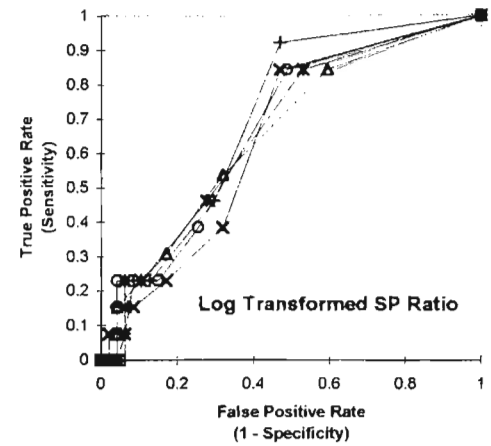

Figure 21. ROC Curves for Log Transformed SP Ratio Method for Class I Obstructions

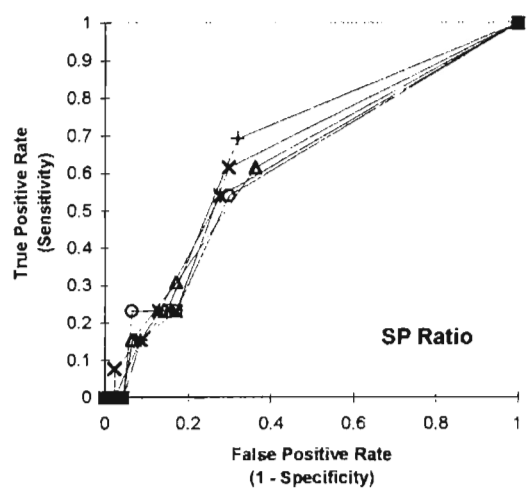

Figure 20. ROC Curves for the SP Ratio Method for Class I Obstructions.

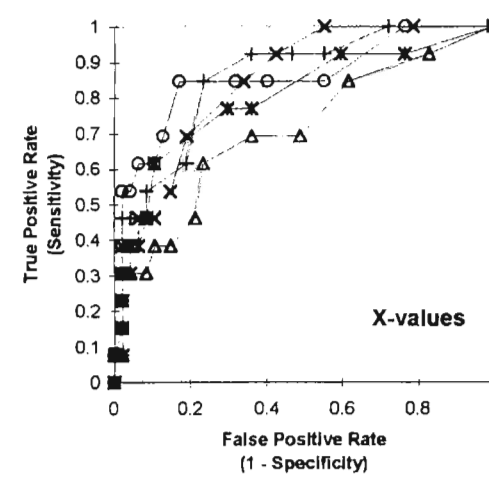

Figure 22. ROC Curves for the X-value Method for Class I Obstructions.

Table 10. Summary of the Area Under the Curves for Each Method for Small (Class I) Obstructions.

Method	Random Draw # 11	12	13	14	15	Mean	St.Dev	Range Min	Max
2-Sided SPH	0.532	0.538	0.525	0.520	0.534	0.530	0.007	0.520	0.538
SP Ratio	0.672	0.630	0.616	0.645	0.625	0.638	0.022	0.616	0.672
Log Trans'd SP Ratio	0.701	0.657	0.673	0.651	0.669	0.670	0.019	0.651	0.701
X-value	0.854	0.705	0.854	0.845	0.799	0.811	0.063	0.705	0.854

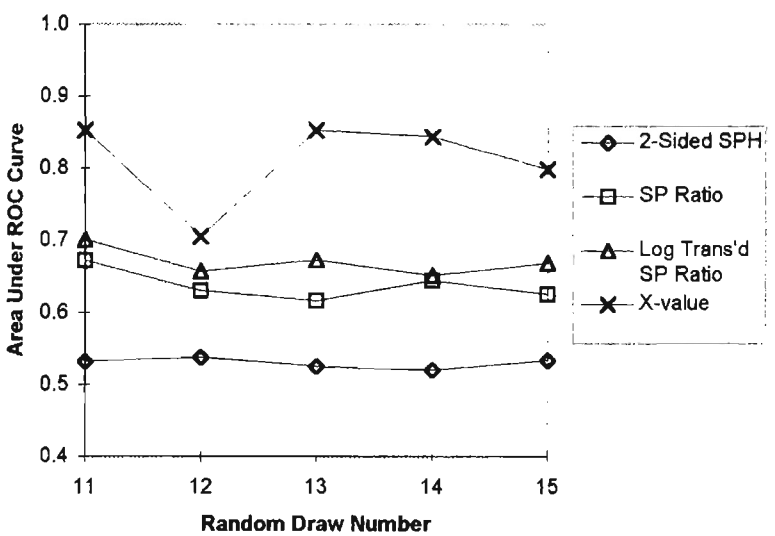

Figure 23. Area Under the Curve Comparisons for Small Obstructions for Each Random Draw.

Summary of the Area Under the ROC Curve Results

The key results from the receiver operating characteristic (ROC) curve analysis of the six troubleshooting methods follow :

- The one-sided SPH and idealized IVM methods performed poorly even on the most severe obstructions.

- The two-sided SPH method consistently had smaller areas under the curves than the SP ratio and X-value methods, indicating a relatively unfavorable combination of sensitivity and false-positive rate.

- For all severities of obstructions, the log transformed SP ratio method consistently out-performed the SP ratio method.

- For moderate obstructions (the main practical concern of ventilation practitioners), the X-value method performed slightly better than any other method.

- The X-value method was much better at identifying the location of small obstructions than other methods.

- The relatively poor performance of the X-value method with severe obstructions was associated with a likely misclassification of a class II obstruction as class III.

Thresholds and False-Positive Rates

The SP ratio methods and the X-value method had nearly the same efficacy for moderate to severe obstructions as ranked by receiver operating characteristic (ROC) curves. Because ROC curve analysis did not lead to a clear choice between the log transformed SP ratio and X-value methods, consideration of acceptable sensitivities and false positive ratios may lead to a clear cut winner. As will be shown, this was not the case – both methods had similar false positive rates for given sensitivities. Because the log transformed SP ratio method does not require time consuming Pitot traverses, it was the better method.

Deciding what is "acceptable" is inherently a policy decision. Poor sensitivity involves costs and ethical issues associated with unremediated alterations, and poor specificity (a high false-positive rate) produces costly unnecessary searches. The important consideration in choosing between the X-value method and the log transformed SP ratio method is balancing the costs of doing a velocity traverse with the costs savings associated with the improved control over the ventilation system.

One way to look at the this tradeoff is to set the sensitivity at a certain level (say 90%) and determine what the threshold needs to be to achieve this. Remember, this corresponds to 10% of the obstructions going undetected. With the threshold set, it is now straight forward to determine the number of costly false positives that will occur. Figure 24 shows a graphical representation of these relationships using an example from the data presented above. To achieve a 90% sensitivity, the X-value threshold needs to be set at around 14%. It should, however, be clear from Figure 24 that there will actually be a range of thresholds depending on which random draw is used. As demonstrated in Figure 25, the log transformed SP ratio method is very similar to the X-value graph (Figure 24), but with a threshold of around 8%. False positive rates for each method are similar, both around 20%.

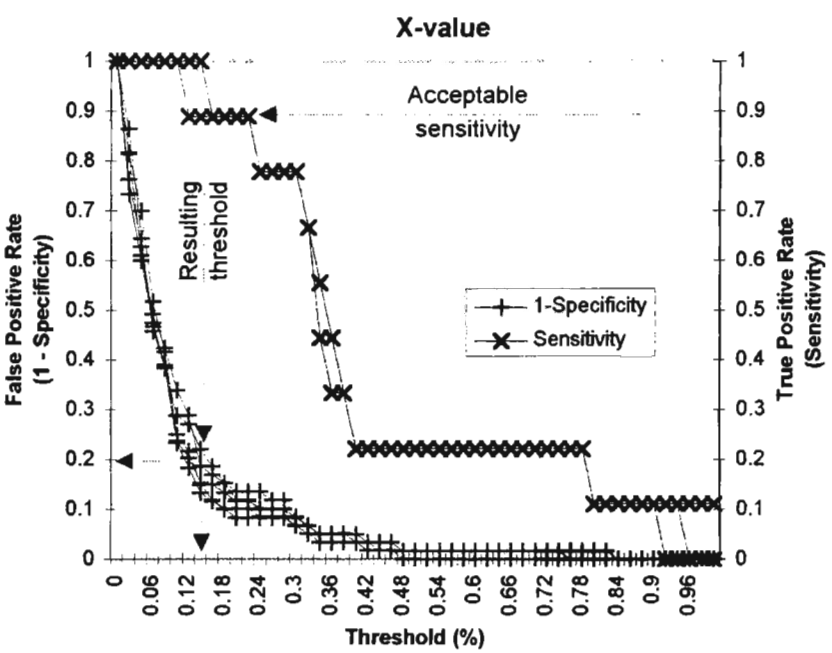

Figure 24. Relationship Between Sensitivity and False Positive Rate as a Function of Threshold for the X-value Method and Class II (Moderate) Obstructions.

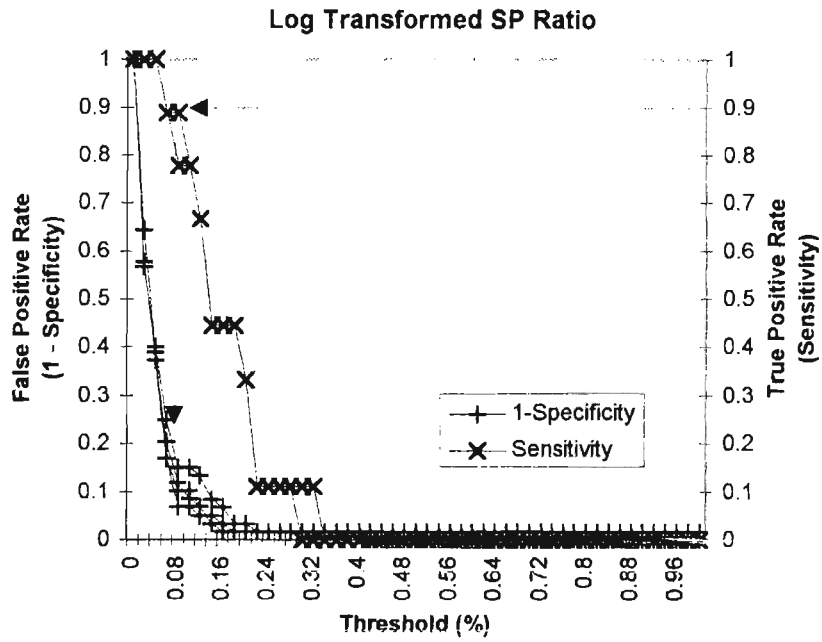

Figure 25. Relationship Between Sensitivity and False Positive Rate as a Function of Threshold for the Log Transformed SP Ratio Method and Class II (Moderate) Obstructions.

To facilitate this analysis, a spreadsheet macro was created which calculated the threshold and false positive rate for a given sensitivity for each of the random draws, methods, and obstruction classes. A linear interpolation was done when the sensitivity and thresholds did not exactly correspond with individual points on the curves. Table 11 presents these results for a 90% sensitivity and Table 12 shows the results for 80% sensitivity. These tables show some consistent trends. First, as the severity of the obstruction decreases, the threshold needed to detect the obstruction decreases as well, and the false-positive rate increases as a result. All methods have a high false positive rate associated with class I obstructions. The probable misclassification of a class III obstruction had a large impact on the observed performance of the method. Accepting a lower sensitivity is associated with a lower false positive rate as one would expect.

Table 12. Thresholds and False-Positive Rates Corresponding to 80% Sensitivity for Each Random Draw by Method and True Obstruction Determination

True Obstruction:	Random Draw #	Two-sided SPH		SP Ratio		Log Trans'd SP Ratio		X-values	
		Threshold	FP Rate	Threshold	FP Rate	Threshold	FP Rate	Threshold	FP Rate
Class III	1	72.4%	11.7%	24.4%	1.7%	56.4%	0.0%	*	0.0%
	2	72.4%	11.7%	22.4%	1.7%	52.4%	0.0%	*	0.0%
	3	70.4%	11.7%	24.4%	1.7%	56.4%	0.0%	*	0.0%
	4	72.4%	11.3%	24.4%	1.7%	54.4%	0.0%	*	0.0%
	5	72.4%	11.3%	24.4%	1.7%	56.4%	0.0%	*	0.0%
Class II Only	1	11.6%	51.2%	3.8%	19.7%	7.6%	8.8%	23.6%	8.5%
	2	9.6%	56.6%	3.8%	23.6%	9.6%	10.5%	23.6%	10.5%
	3	11.6%	53.6%	3.8%	18.8%	9.6%	10.2%	23.6%	10.2%
	4	11.6%	53.9%	3.8%	25.3%	7.6%	13.6%	23.6%	13.6%
	5	10.5%	52.5%	3.8%	20.2%	9.6%	10.2%	23.6%	8.8%
Class I Only	1	5.6%	63.8%	1.3%	55.7%	2.5%	42.3%	10.4%	22.6%
	2	5.6%	65.1%	1.0%	66.8%	2.3%	55.4%	4.6%	57.9%
	3	5.6%	63.8%	0.9%	69.6%	2.2%	46.6%	10.6%	15.7%
	4	5.6%	66.0%	1.0%	63.5%	2.2%	45.3%	8.6%	29.6%
	5	5.6%	68.1%	0.9%	68.7%	2.2%	50.1%	5.6%	40.9%

* A 0% threshold will not achieve a 80% sensitivity, therefore no thresholds or false-positive rates can be given.

Table 11. Thresholds and False-Positive Rates Corresponding to 90% Sensitivity for Each Random Draw by Method and True Obstruction Determination

True Obstruction:	Random Draw #	Two-sided SPH		SP Ratio		Log Trans'd SP Ratio		X-values	
		Threshold	FP Rate	Threshold	FP Rate	Threshold	FP Rate	Threshold	FP Rate
Class III	1	9.2%	59.0%	11.2%	1.7%	23.2%	1.7%	11.2%	21.0%
	2	9.2%	59.3%	11.2%	1.7%	23.2%	1.7%	11.2%	27.7%
	3	9.2%	58.7%	11.2%	1.7%	23.2%	1.7%	17.2%	13.0%
	4	9.2%	60.0%	11.2%	1.7%	23.2%	1.7%	17.2%	11.3%
	5	9.2%	62.0%	11.2%	1.7%	23.2%	1.7%	11.2%	31.0%
Class II Only	1	7.8%	62.9%	2.9%	31.9%	5.8%	19.2%	15.8%	12.2%
	2	7.8%	59.8%	2.9%	30.4%	5.8%	20.3%	15.8%	19.0%
	3	7.8%	65.1%	2.9%	27.2%	5.8%	15.3%	15.8%	11.9%
	4	7.8%	64.6%	2.9%	32.1%	5.8%	22.0%	15.8%	17.1%
	5	7.8%	58.1%	2.9%	27.0%	5.8%	19.0%	11.8%	20.7%
Class I Only	1	4.3%	70.7%	0.7%	77.9%	2.1%	46.0%	8.6%	32.3%
	2	4.3%	69.3%	0.5%	83.4%	1.3%	73.7%	2.6%	76.6%
	3	4.3%	70.7%	0.4%	84.8%	1.3%	66.8%	3.3%	62.8%
	4	4.3%	72.9%	0.5%	81.7%	1.3%	65.4%	6.6%	40.0%
	5	4.3%	75.0%	0.4%	84.3%	1.3%	69.6%	4.3%	56.1%

* A 0% threshold will not achieve a 90% sensitivity, therefore no thresholds can be given.

Because the log transformed SP ratio method and the X-value method were determined to be similar in performance with respect to ROC curves, the direct comparison of their false positive rates at a given threshold is of particular importance. Table 13 shows this comparison for class II obstructions, the ones that are probably of most interest to ventilation practitioners.

Table 13. Comparison of Thresholds and False-Positive Rates for the Log Transformed SP Ratio and the X-value Methods for Class II obstructions

	Log Transformed SP Ratio		X-value	
Sensitivity	Threshold Range	FP Rate Range	Threshold Range	FP Rate Range
90%	5.8%	15.3 - 22.0%	11.9 - 15.8%	11.9 - 20.7%
80%	7.6 - 9.6%	8.8 - 13.6%	23.6%	8.5 - 13.6%

Hoppe (1995) showed that a 17% shift in X-value was associated with a 5% shift in airflow. Though these results are somewhat dependent on the system used, the implications as to the degree of control that is possible is particularly interesting. Thus, a 90% sensitivity was associated with a degree of control over the airflow of each branch of just under 5%; whereas at an 80% sensitivity, the smallest change that could be detected was slightly higher than 5%.

There appears to be no substantial and consistent difference in false-positive rates between the log transformed SP ratio and X-value methods at two different sensitivities (Table 13). Thus, it appears that the difference between the two methods in terms of their ROC curve performance occurs at lower sensitivities that may be of little concern to ventilation practitioners who are interested in identifying only obstructions that substantially affect air flow. Because the X-value method requires time and cost intensive velocity traverses, the overall preferred method for troubleshooting branches is the log transformed SP ratio method. However, the log transformed static pressure ratio method cannot be used on submains. If an obstruction is suspected in the submain, X-values or a sophisticated interpretation of adjacent hood static pressures needs to be used (Guffey, 1994).

Limitations and Research Needs

As previously stated, these results are based on a limited number of obstructions, seven for class II and six for class III. For each of the obstructions, however, repeat measurements were frequently made which allowed a testing of the consistency of the results. These repeat measurements were incorporated into the analysis by doing a random draw from the set of possible comparisons between baseline and altered states for an individual duct. These total possible comparisons totaled 18 for class II obstructions and 24 for class III obstructions. This random draw was repeated five times, yielding five different ROC curves. However, ultimately the results are still based on less than nine different obstructions. The study could have achieved more power and better ability to at discern differences among the methods by having a larger sample size for each of the obstruction classifications. Practical limitations precluded this. Additional repeat draws on the data did not yield different conclusions.

The performance of X-values relative to the other methods may be dependent on the ventilation system measured. If the system has only good traverse locations which allow for an accurate characterization of velocity pressures, the X-value method may well have performed much better than the log transformed SP ratio method. Because of the limited number of systems that could be investigated over the course of this study, this relationship could not be addressed

However, it is reasonable to assume that ideal measurement conditions will not exist for most ventilation systems because of limited space in most industrial facilities. As was the case at Blum Saw, it is frequently necessary for even short branches to have several 90 degree bends before they join a submain. This makes accurate and precise velocity pressure traverses challenging at best because the airflow does not have enough time to stabilize. A second, perpendicular traverses may help, but at the cost of additional time and effort. Additional work is needed to see whether perpendicular velocity traverses substantially improve the performance of X-values. Also, since low pressures are more difficult to measure precisely than high velocities, the precision and usefulness of X-values may depend on duct velocities. This question is left to future research.

The location of the obstruction may also affect the efficacy of log transformed SP ratio and X-value methods. One method may be better at picking out the alterations that occur at the hood and another better at finding ones that occur between hood and the end. If for example, it is known that no obstructions occur between the hood opening and the hood measurement location (SPH), one might choose one method over another because it is more sensitive to these types of alterations and produces fewer false positives.

Care needs to be taken when using the log transformed SP ratio method on other ventilation systems. The constant, "1.2," used in the log transformation equation (equation 12) was based on the largest observed static pressure ratio. Depending on the location and variability of measurement locations, other systems may have a higher or lower maximum static pressure ratio. Thus, a constant other than 1.2 may be appropriate when using the log transformed SP ratio. Further work is needed to see how the log transformed SP ratio method performs relative to the other methods when a different constant is used.

As was mentioned earlier, there is a potential problem with misclassification of the obstructions into the four obstruction classes. Obstructions occur in a continuous spectrum of sizes such that they do not naturally fall into the arbitrary categories of percent of the duct area blocked (0%, 0-20%, 20-60%, and 60-100%). Some degree of misclassification is likely at the cutoffs. Improvement in the ability of future researchers to estimate the percent of the duct area that is blocked may improve this. However, it will be difficult to quantify other factors associated with each obstruction such as shape and the effect of being close to an elbow.

CHAPTER 4 – CONCLUSIONS

The goal of this study was to determine which of the proposed troubleshooting methods were better at identifying a range of obstructions found in the field. To ensure the consistency of the conclusions, several repeat rounds of measurements were done and used in the preparation of the receiver operating characteristic curves (ROC curves).

The one-sided SPH and idealized IVM methods were clearly inadequate, in part due to their inability to detect obstructions that occur between the hood opening and the hood measurement location. The two-sided SPH method did not suffer that limitation, but still performed significantly worse over all obstruction classifications than the two methods based on SP ratios and the X-value method. The log transformed SP ratio method always did better than the SP ratio method. This was likely because of its ability to detect smaller changes when the static pressure ratio is large (i.e., cases where the hood accounts for the majority of the pressure loss for the whole branch). The comparison between X-values and static pressure ratios had mixed findings.

For moderate obstructions – those of most concern to ventilation practitioners – X-value method had a consistently slightly larger area under the ROC curve than the log transformed SP ratio method. For small obstructions, the X-values had significantly larger areas under the ROC curves. Thus, the X-value method may be the correct choice if there is a need to have tight control on the functioning of the ventilation system (and the company can afford a false-positive rate of 30 - 75% for a 90% sensitivity).

No significant between X-value and log transformed SP ratio methods was shown when "acceptable" sensitivities were considered. For a sensitivity of 80%, each method had similar false-positive rates in the range of 12 to 22%, and 8 to 15% for 80% sensitivity.

Given similar performance of these two methods, the overall conclusion from this data is that the better method is the log transformed static pressure ratio method because the X-value

method requires time-consuming velocity traverses. However, if obstructions are suspected in the submains, then the log transformed SP ratio cannot be used, but X-values can. More work is needed to determine the efficacy of X-values in finding submain alterations.

It may be presumptuous to generalize the findings because of the relatively few number of obstructions that were observed. This conclusion was based on only seven different obstructions and should be tested with a larger number of class II obstructions before wide-spread adoption. In addition, the study only addressed obstructions. Further research is needed to determine which method is best at identifying leaks.

All methods studied are contingent on "before" and "after" rounds of measurements. Only the *Industrial Ventilation Manual* method can be used without baseline data, and even an idealized version of this method was shown to be ineffective even with severe obstructions. Use of loss coefficients further degrades its reliability. However in some circumstances, this is the only feasible method if there is no baseline data available.

For future research, it is highly recommended that a data logging system like what was used in this study be used. Not only does it reduce mathematical and transcription errors, but it also helps to eliminate bias and save a substantial amount of time.

LIST OF REFERENCES

Alden, John, and John M. Kane. *Design of Industrial Ventilation Systems,* 5th ed. New York: Industrial Press, 1982.

Alnor Instrument Company. "CompuFlow ElectroManometer Model 8530D-I Owner's Manual" (#116-159-035 Rev. 2), Skokie, IL, 1987.

_____. "CompuFlow RS232 Interface Module Owner's Manual" (#116-159-020), Skokie, IL, 1986.

American Conference of Governmental Industrial Hygienists. *Industrial Ventilation: A Manual of Recommended Practice.* 22d ed. Lansing, MI: ACGIH, 1994.

American Society of Heating Refrigerating and Air-Conditioning Engineers. *ASHRAE Handbook -- 1989 Fundamentals.* Atlanta, GA: ASHRAE, 1989.

Baturin, V. V. *Fundamentals of Industrial Ventilation,* 3d ed. Translated by O. M. Blunn. New York: Pergamon, 1972.

Beck, J. Robert, and Edward K. Shultz. "The Use of Relative Operating Characteristic (ROC) Curves in Test Performance Evaluation." *Arch. Pathol. Lab. Med.* 110 (Jan 1986): 13 - 20.

Burgess, William A., Michael Ellenbecker, and Robert Treitman. *Ventilation for Control of the Work Environment.* New York: John Wiley, 1989.

Burton, D. Jeff. Industrial Ventilation: A Self Study Companion to the ACGIH Ventilation Manual. Salt Lake City, UT: Jeff Burton, 1982.

Cleary, William. Personal communication, 4/3/96

Colvin, Scott C. "Experimental Validation of the Efficacy of Power Loss Coefficients in Detecting Ventilation System Modifications and in Predicting New Airflow Levels and Pressures." MS thesis, Department of Environmental Health, University of Washington, 1993.

Guffey, Steven E. *Heavent Owner's Manual.* Seattle, WA: Steven E. Guffey, 1996.

_____. "Quantitative Troubleshooting of Industrial Exhaust Ventilation Systems." *Appl. Occup. Environ. Hyg.* 9, no. 4 (1994): 267 - 80.

_____. "Air-Flow Redistribution in Exhaust Ventilation Systems Using Dampers and Static Pressure Ratios." *Appl. Occup. Environ. Hyg.* 8, no. 3 (1993a): 168 - 177.

_____. "Modeling Existing Ventilation Systems Using Measured Values," *Am. Ind. Hyg. Assoc. J.* 54 (June 1993b): 293 - 305.

_____. "Simplifying Pitot Traverses." *App. Occup. Environ. Hyg.* 5, no. 2 (1990): 95 - 100.

Guffey, S. E. and D. A. Fraser. "A Power Balance Model for Converging and Diverging Flow Junctions." *ASHRAE Transactions* (1988)

Hoppe, Jeanne. "Empirical Determination of the Error in the ACGIH Method of Predicting Airflow Distribution in Two Industrial Ventilation Systems." MS thesis, Department of Environmental Health, University of Washington, 1995.

McDermott, H. J. *Handbook for Ventilation for Contaminant Control*, 2d ed. Boston: Butterworth, 1985.

Metz, Charles E. "Basic Principles of ROC Analysis." *Seminars in Nuclear Medicine* 8, no. 4 (1978): 283 - 98.

Pinsky, Ann. "Comparison of Efficacies of Current Methods for Troubleshooting Industrial Exhaust Ventilation Systems to a Proposed New Method." MS thesis, Department of Environmental Health, University of Washington, 1996.

Ower, E, and R. C. Pankhurst. *The Measurement of Air Flow*, 5th ed. New York: Pergamon, 1977.

Spann, Jeffrey G. "Experimental Investigation of Power Loss Coefficients and Static Pressure Ratios in an Industrial Exhaust Ventilation System." MS thesis, Department of Environmental Health, University of Washington, 1993.

APPENDIX A – CALIBRATION

The complete calibration data from the calibration of the Alnor® Electromanometer and the Meriam® Inclined Manomoter appears at the end of this Appendix as Table 14.

Calibration of the Alnor® Electromanometer and the inclined manometer during the course of the study against the Dwyer® hook gage (a primary standard) originally yielded differences as high as 10%. It was later determined that this was likely due to inconsistencies in technique. Seeing the point of the caliper pierce the top of the fluid was originally how the level differences were determined, but significant amount of variability. On May 1, 1996, a more precise method of marking the level change was used. This relied on reading the value when the water surface deflects to the tip of the caliper just below the surface. Figure 26 shows a graph of the difference between the inclined and the micromanometer. Note that there is a slight gain. This is likely due to a slight error in the original calibration of the inclined manometer or in minor changes over time. Because this is likely consistent throughout the data and the main variable in the study is relative change, this gain error should have little impact on the conclusions of the study. Note that even with the gain error, the deviation is no more than 0.03 at 4 in.w.g. or 0.75%.

The calibration between the Alnor® and the inclined manometer was consistent over the range of data used in this study; only once did they differ by more than 0.01 in.w.g. (see

Figure 27).

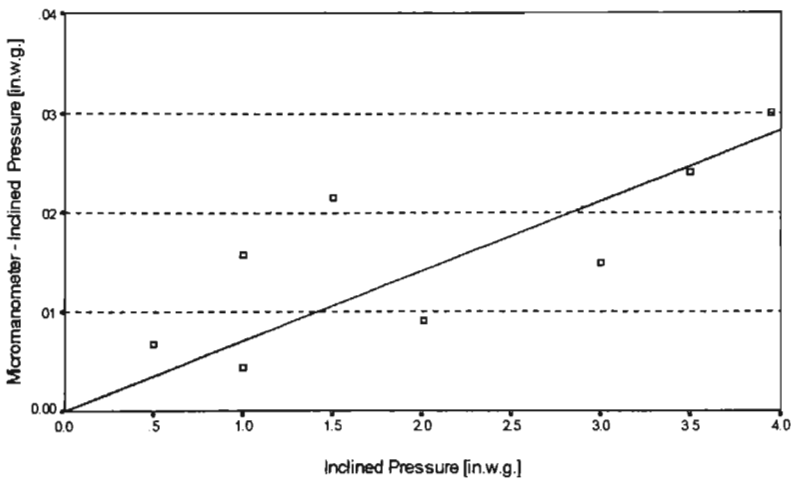

Figure 26. Pressure Difference Between Inclined Manometer to the Micromanometer During Calibration on May 1, 1996.

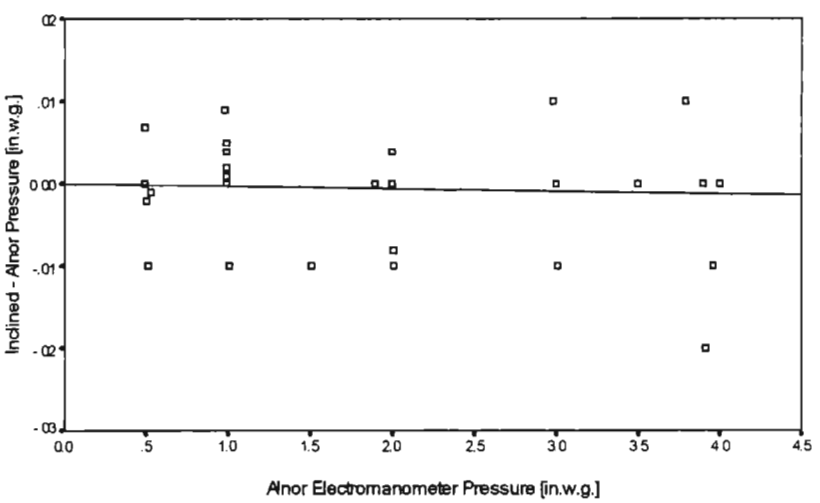

Figure 27. Pressure Difference Between the Alnor® Electromanometer and the Inclined Manometer During Calibration.

Table 14. Calibration Data

Date	Alnor ["w.g.] (1)	Inclined ["w.g.] (2)	Micromanometer ["w.g.] (3)
1/18/96	0.502	0.500	
1/18/96	0.991	1.000	
1/18/96	2.00	2.000	
1/18/96	2.99	3.000	
1/18/96	4.00	4.000	
2/2/96	0.502	0.500	
2/2/96	0.999	1.000	
2/2/96	2.00	2.000	
2/2/96	2.99	3.000	
2/2/96	3.79	3.800	
3/5/96	0.530	0.529	
3/5/96	1.00	1.004	
3/5/96	2.01	2.002	
3/5/96	3.00	3.000	
3/5/96	4.00	4.000	
3/18/96	0.51	0.500	
3/18/96	1.01	1.000	
3/18/96	2.01	2.000	
3/18/96	3.01	3.000	
3/18/96	3.92	3.900	
4/5/96	0.493	0.500	
4/5/96	0.995	1.000	
4/5/96	1.90	1.900	
4/5/96	2.99	3.000	
4/5/96	3.90	3.900	
5/1/96	0.50	0.500	0.5068
5/1/96	1.00	1.000	1.0044
5/1/96	1.51	1.500	1.5216
5/1/96	2.00	2.004	2.0130
5/1/96	3.00	3.000	3.0150
5/1/96	3.50	3.500	3.5240
5/1/96	3.96	3.950	3.9800
5/1/96	1	1.002	1.0178

(1) Alnor = Alnor® Compuflow Electromanometer 8530d-I (S# 004852)

(2) Inclined = Meriam® Instrument Model 40HE35WM (S# 149990C1)

(3) Micromanometer = Dwyer® Instruments Hook Gage (Series 1425)

APPENDIX B – EQUATION DERIVATIONS

Derivation of $\frac{X_{hood}+1}{X_{end}+1}=\frac{SPH}{SP_{end}}$

$$\frac{X_{hood}+1}{X_{end}+1}=\frac{-\frac{TP_{hood}}{VP_{br}}+1}{-\frac{TP_{end}}{VP_{br}}+1}=\frac{\frac{-TP_{hood}+VP_{br}}{VP_{br}}}{\frac{-TP_{end}+VP_{br}}{VP_{br}}}=\frac{-TP_{hood}+VP_{br}}{-TP_{end}+VP_{br}}$$

Substituting in TP = SP + VP (where SP is a negative number) yeilds:

$$\frac{-TP_{hood}+VP_{br}}{-TP_{end}+VP_{br}}=\frac{\left(-SP_{hood}-VP_{br}\right)+VP_{br}}{\left(-SP_{end}-VP_{br}\right)+VP_{br}}=\frac{SP_{hood}}{SP_{end}}$$

APPENDIX C – EQUIPMENT USED

Alnor Compuflow Electromanometer 8530d-I (S# 004852)

Meriam Instrument Model 40HE35WM (S# 149990C1)

Dwyer Instruments Hook Gage (S# 1425)

1/8 inch Dwyer stainless steel pitot tube with a 1.5 inch lead tube, Model 167-6

Hewlett Packard 100LX Palmtop PC w/2 MB RAM.

Prolinear MiniNote palmtop computer, Model ME-386 (Prolinear Corp., Arcadia, CA)

Alnor CompuFlow ElectroManometer, model 8530D-I. (Skokie, IL)

Alnor RS232 Datalogging Module, SN 1194 (Skokie, IL)

Borescope, Series 5, (Olympus America, Melville, NY)

Light Source, Olympus ILK-5 (Olympus of America, Lake Success, NY)

Viewing adapter, Olympus AK2-18-90 (Olympus of America, Lake Success, NY)

Toshiba Portege Model T3400 Laptop Computer (SN 0243171)

HV_MEAS Pressure Measurement Spreadsheet Software

Dwyer 1/8" Pitot Tube, 12" long

Tygon® Tubing

Plastic Couplers for Tygon Tubing

Flashlight

DeWalt Cordless 3/8" VSR Drill

Fowler Instruments 12" Micrometer (SN 6904096)

Safety glasses & hearing protection

Duct tape, colored labeling tape

APPENDIX D – BACKGROUND ON ROC CURVES

Troubleshooting analysis is similar to a the analysis of a medical screening tool – which screening method most accurately predicts which people are diseased and which are not. In this study, the question being answered is which screening method most accurately predicts the "diseased" duct. In doing this analysis, it is common practice to construct contingency tables as shown in Figure 28 to aid the data interpretation.

Sensitivity is defined as the percent of the total true alterations that were indicated by the screening method to be true. A good screening tool would identify 100% of the true alterations; however, if the screening tool identified all alterations as being true without discerning those that are truly false, its utility is questionable. Specificity is another metric in this screening tool analysis that gets at this question. Specificity is defined as the percent of the truly negative observations which were indicated as such by the screening tool. Like sensitivity, a good screening tool will have a specificity near 100%. The ideal screening tool will have a sensitivity of 100% and a specificity of 100%.

It should be clear that sensitivity and specificity are strongly tied to the threshold that is used in the classification of suspected alterations. In the analysis for this study, the relative change of a troubleshooting method's decision variable (e.g., SPH, SP ratios, X-value) is computed between two sets of measurements. If the relative change of the decision variable is greater than some threshold, then an alteration is suspected.

Because the sensitivities and specificities vary depending on the threshold that is chosen, it is necessary to integrate these three variables in an analysis to reach a conclusion about which one is better. Receiver operating characteristic curves do this (Beck & Shultz, 1986; Metz, 1978). The true positive rate (sensitivity) is plotted against the false positive rate (1 - specificity) as shown in Figure 29. The better method is the one that reaches a high sensitivity with the fewest

false positives. In other words, the better method is the one which is higher and to the left. In the example below, method B is superior to method A.

		Truth (duct inspection)	
		Alteration found (+)	Alteration not found (-)
Screening Method	Alteration suspected (+)	TP	FP
	No alteration suspected (-)	FN	TN
		Total number of true alterations	Total number of false alterations

$$\text{Sensitivity} = \frac{TP}{TP + FN}; \qquad \text{Specificity} = \frac{TN}{FP + TN}$$

TP = true positive
TN = true negative
FP = false positive
FN = false negative

Figure 28. Contingency Table to calculate the Sensitivity and Specificity of Each Method Given a Specific Decision Threshold

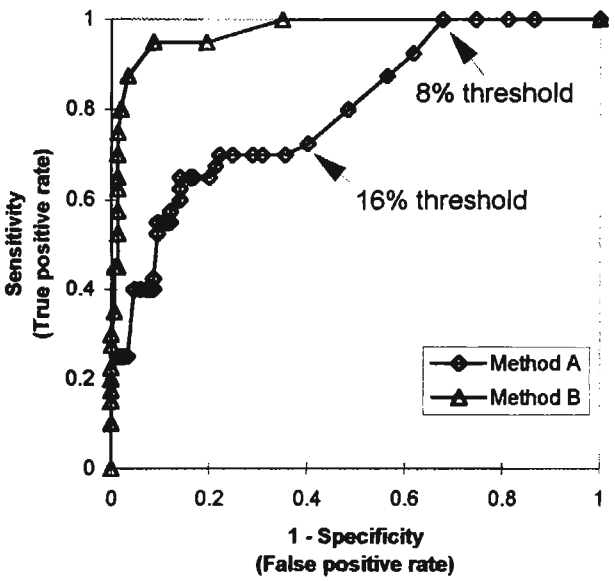

Figure 29. Sample comparison of ROC curves. The better method has the larger area under the curve and, thus, is higher and to the left in the above diagram.

The better method is also shown by the larger area under the ROC curve. This area has been shown to be mathematically equivalent to the probability that, given two branches, one normal and one obstructed, the troubleshooting test result will indicate a "more obstructed" branch in the obstructed branch (Beck & Shultz, 1986).

APPENDIX E – LIST OF COMPARISONS

This is a list of baseline/altered comparisons from which the change in troubleshooting variables were calculated. The repeat group category is a categorization of comparisons which should have the same change in troubleshooting variables. Random draws on the data are made within the repeat group category (i.e., there will only be one "a," one "b," etc.).

Duct ID	Base-line file:	Altered file:	Change noted? Describe.	Repeat group	Obstruc-tion Class	Alteration upstream of SPH?	Same day meas?
13	bs9602b1	bs9602a3	Removed 2 cups of dust and clumps from the hood flex duct.	a	2	Y	Y
13	bs9602b2	bs9602a3	Removed 2 cups of dust and clumps from the hood flex duct.	a	2	Y	Y
23	bs9602b1	bs9602a1	SG fixed bent duct and cleaned out ~1/8 C of dust and clumps @ elbow area to vertical.	b	1	N	Y
23	bs9602b2	bs9602a1	SG fixed bent duct and cleaned out ~1/8 C of dust and clumps@ elbow area to vertical.	b	1	N	Y
23	bs9602b1	bs9602a2	SG fixed bent duct and cleaned out ~1/8 C of dust and clumps @ elbow area to vertical.	b	1	N	Y
23	bs9602b2	bs9602a2	SG fixed bent duct and cleaned out ~1/8 C of dust and clumps @ elbow area to vertical.	b	1	N	Y
33	bs9602b1	bs9602a1	Rag caught in duct bet hood flex and floor. ~2 c in hood. 1/4 C dwnstrm of elbow.	c	3	N	Y
33	bs9602b2	bs9602a1	Rag caught in duct bet hood flex and floor. ~2 c in hood. 1/4 C dwnstrm of elbow.	c	3	N	Y
33	bs9602b1	bs9602a2	Rag caught in duct bet hood flex and floor. ~2 c in hood. 1/4 C dwnstrm of elbow.	c	3	N	Y
33	bs9602b2	bs9602a2	Rag caught in duct bet hood flex and floor. ~2 c in hood. 1/4 C dwnstrm of elbow.	c	3	N	Y
43	bs9602b1	bs9602a2	Hood almost fully blocked. ~2 C of clumps in flex of hood. dwnstrm, a few thumbsized clumps were removed from longer metal duct.	d	3	Y	Y
43	bs9602b2	bs9602a2	Hood almost fully blocked. ~2 C of clumps in flex of hood. dwnstrm, a few thumbsized clumps were removed from longer metal duct.	d	3	Y	Y
43	bs9602b1	bs9602a3	Hood almost fully blocked. ~2 C of clumps in flex of hood. dwnstrm, a few thumbsized clumps were removed from longer metal duct.	d	3	Y	Y
43	bs9602b2	bs9602a3	Hood almost fully blocked. ~2 C of clumps in flex of hood. dwnstrm, a few thumbsized clumps were	d	3	Y	Y

			removed from longer metal duct.				
53	bs9602b1	bs9602a1	~1/8 C dwnstrm of Spen left in. 3 clumps bet mid and end removed.	e	1	N	Y
53	bs9602b2	bs9602a1	~1/8 C dwnstrm of Spen left in. 3 clumps bet mid and end removed.	e	1	N	Y
53	bs9602b1	bs9602a2	~1/8 C dwnstrm of Spen left in. 3 clumps bet mid and end removed.	e	1	N	Y
53	bs9602b2	bs9602a2	~1/8 C dwnstrm of Spen left in. 3 clumps bet mid and end removed.	e	1	N	Y
63	bs9602b1	bs9602a1	Hood fully blocked (3-4 C). Mid to end had ~`1T which should affect pressures.	f	3	Y	Y
63	bs9602b2	bs9602a1	Hood fully blocked (3-4 C). Mid to end had ~`1T which should affect pressures.	f	3	Y	Y
63	bs9602b1	bs9602a2	Hood fully blocked (3-4 C). Mid to end had ~`1T which should affect pressures.	f	3	Y	Y
63	bs9602b2	bs9602a2	Hood fully blocked (3-4 C). Mid to end had ~1 T which should affect pressures.	f	3	Y	Y
73	bs9602b1	bs9602a1	1/3 - 1/2 blocked @ hood entrance (~3 C). 1 T in elbow to submain which shouldn't affect pressures.	g	2	Y	Y
73	bs9602b2	bs9602a1	1/3 - 1/2 blocked @ hood entrance (~3 C). 1 T in elbow to submain which shouldn't affect pressures.	g	2	Y	Y
73	bs9602b1	bs9602a2	1/3 - 1/2 blocked @ hood entrance (~3 C). 1 T in elbow to submain which shouldn't affect pressures.	g	2	Y	Y
73	bs9602b2	bs9602a2	1/3 - 1/2 blocked @ hood entrance (~3 C). 1 T in elbow to submain which shouldn't affect pressures.	g	2	Y	Y
83	bs9603b1	bs9603a1	Clean	h	0	N	Y
83	bs9603b2	bs9603a1	Clean	h	0	N	Y
83	bs9603b1	bs9603a2	Clean	h	0	N	Y
83	bs9603b2	bs9603a2	Clean	h	0	N	Y
93	bs9603b1	bs9603a2	Clean	i	0	N	Y
93	bs9603b2	bs9603a2	Clean	i	0	N	Y
93	bs9603b1	bs9603a3	Clean	i	0	N	Y
93	bs9603b2	bs9603a3	Clean	i	0	N	Y
103	bs9603b1	bs9603a1	Practically clean both times, but 10 stellite tips b4 vertical.	j	0	N	Y
103	bs9603b2	bs9603a1	Practically clean both times, but 10 stellite tips b4 vertical.	j	0	N	Y
103	bs9603b1	bs9603a2	Practically clean both times, but 10 stellite tips b4 vertical.	j	0	N	Y
103	bs9603b2	bs9603a2	Practically clean both times, but 10 stellite tips b4 vertical.	j	0	N	Y
113	bs9603b1	bs9603a1	Clean	k	0	N	Y
113	bs9603b2	bs9603a1	Clean	k	0	N	Y
113	bs9603b1	bs9603a2	Clean	k	0	N	Y
113	bs9603b2	bs9603a2	Clean	k	0	N	Y
123	bs9603b1	bs9603a1	~1/2 blocked at hood bottleneck	l	2	Y	Y
123	bs9603b2	bs9603a1	~1/2 blocked at hood bottleneck	l	2	Y	Y
123	bs9603b1	bs9603a2	Clean	l	2	Y	Y
123	bs9603b2	bs9603a2	Clean	l	2	Y	Y
13	bs9602b1	bs960319	modest coating upstrm of SPH.	m	1	Y	N
13	bs9602b2	bs960319	modest coating upstrm of SPH.	m	1	Y	N
23	bs9602b1	bs960319	modest clumps at opening to hood. Some light coating upstram of hood.	n	1	Y	N
23	bs9602b2	bs960319	modest clumps at opening to hood. Some light coating upstram of hood.	n	1	Y	N
33	bs9602b1	bs960319	Clean but for one small clump in the	o	1	Y	N

			flex.				
33	bs9602b2	bs960319	Clean but for one small clump in the flex.	o	1	Y	N
43	bs9602b1	bs960319	Between modest and moderate clumps upstream of SPH.	p	1	Y	N
43	bs9602b2	bs960319	Between modest and moderate clumps upstream of SPH.	p	1	Y	N
53	bs9602b1	bs960319	V. modest accumulation upstream of SPH.	q	1	Y	N
53	bs9602b2	bs960319	V. modest accumulation upstream of SPH.	q	1	Y	N
63	bs9602b1	bs960319	modest clumps dwnstrm of Spen. Modest clumps and settling uptrm of SPH.	r	1	Y	N
63	bs9602b2	bs960319	modest clumps dwnstrm of Spen. Modest clumps and settling uptrm of SPH.	r	1	Y	N
73	bs9602b1	bs960319	clean	s	0	N	N
73	bs9602b2	bs960319	clean	s	0	N	N
83	bs9603b1	bs960319	clean	t	0	N	N
83	bs9603b2	bs960319	clean	t	0	N	N
83	bs9603b1	bs9603f1	Repeat after full system measurement.	t	0	N	N
83	bs9603b2	bs9603f1	Repeat after full system measurement.	t	0	N	N
93	bs9603b1	bs960319	clean	u	0	N	N
93	bs9603b2	bs960319	clean	u	0	N	N
93	bs9603b1	bs9603f1	Repeat after full system measurement.	u	0	N	N
93	bs9603b2	bs9603f1	Repeat after full system measurement.	u	0	N	N
103	bs9603b1	bs960319	clean	v	0	N	N
103	bs9603b2	bs960319	clean	v	0	N	N
103	bs9603b1	bs9603f1	Repeat after full system measurement.	v	0	N	N
103	bs9603b2	bs9603f1	Repeat after full system measurement.	v	0	N	N
113	bs9603b1	bs960319	clean	w	0	N	N
113	bs9603b2	bs960319	clean	w	0	N	N
113	bs9603b1	bs9603f1	Repeat after full system measurement.	w	0	N	N
113	bs9603b2	bs9603f1	Repeat after full system measurement.	w	0	N	N
123	bs9603b1	bs960319	clean	x	0	N	N
123	bs9603b2	bs960319	clean	x	0	N	N
123	bs9603b1	bs9603f1	Repeat after full system measurement.	x	0	N	N
123	bs9603b2	bs9603f1	Repeat after full system measurement.	x	0	N	N
13	bs9603g1	bs9603h1	Clean. Increased airflow by putting woodstrip in 23 and blocking 113, 123, 133.	y	0	N	Y
13	bs9603g2	bs9603h1	Clean. Increased airflow by putting woodstrip in 23 and blocking 113, 123, 133.	y	0	N	Y
13	bs9603g1	bs9603h2	Clean. Increased airflow by putting woodstrip in 23 and blocking 113, 123, 133.	y	0	N	Y
13	bs9603g2	bs9603h2	Clean. Increased airflow by putting woodstrip in 23 and blocking 113, 123, 133.	y	0	N	Y
23	bs9603g1	bs9603h1	entrance blocked with wood strip. Increased airflow by putting woodstrip in 23 and blocking 113,	z	2	Y	Y

			123, 133.				
23	bs9603g2	bs9603h1	entrance blocked with wood strip. Increased airflow by putting woodstrip in 23 and blocking 113, 123, 133.	z	2	Y	Y
23	bs9603g1	bs9603h2	entrance blocked with wood strip. Increased airflow by putting woodstrip in 23 and blocking 113, 123, 133.	z	2	Y	Y
23	bs9603g2	bs9603h2	entrance blocked with wood strip. Increased airflow by putting woodstrip in 23 and blocking 113, 123, 133.	z	2	Y	Y
33	bs9603g1	bs9603h1	Clean. Increased airflow by putting woodstrip in 23 and blocking 113, 123, 133.	aa	0	N	Y
33	bs9603g2	bs9603h1	Clean. Increased airflow by putting woodstrip in 23 and blocking 113, 123, 133.	aa	0	N	Y
33	bs9603g1	bs9603h2	Clean. Increased airflow by putting woodstrip in 23 and blocking 113, 123, 133.	aa	0	N	Y
33	bs9603g2	bs9603h2	Clean. Increased airflow by putting woodstrip in 23 and blocking 113, 123, 133.	aa	0	N	Y
43	bs9603g1	bs9603h1	Clean. Increased airflow by putting woodstrip in 23 and blocking 113, 123, 133.	bb	0	N	Y
43	bs9603g2	bs9603h1	Clean. Increased airflow by putting woodstrip in 23 and blocking 113, 123, 133.	bb	0	N	Y
43	bs9603g1	bs9603h2	Clean. Increased airflow by putting woodstrip in 23 and blocking 113, 123, 133.	bb	0	N	Y
43	bs9603g2	bs9603h2	Clean. Increased airflow by putting woodstrip in 23 and blocking 113, 123, 133.	bb	0	N	Y
53	bs9603g1	bs9603h1	Clean. Increased airflow by putting woodstrip in 23 and blocking 113, 123, 133.	cc	0	N	Y
53	bs9603g2	bs9603h1	Clean. Increased airflow by putting woodstrip in 23 and blocking 113, 123, 133.	cc	0	N	Y
53	bs9603g1	bs9603h2	Clean. Increased airflow by putting woodstrip in 23 and blocking 113, 123, 133.	cc	0	N	Y
53	bs9603g2	bs9603h2	Clean. Increased airflow by putting woodstrip in 23 and blocking 113, 123, 133.	cc	0	N	Y
63	bs9603g1	bs9603h1	Clean. Increased airflow by putting woodstrip in 23 and blocking 113, 123, 133.	dd	0	N	Y
63	bs9603g2	bs9603h1	Clean. Increased airflow by putting woodstrip in 23 and blocking 113, 123, 133.	dd	0	N	Y
63	bs9603g1	bs9603h2	Clean. Increased airflow by putting woodstrip in 23 and blocking 113, 123, 133.	dd	0	N	Y
63	bs9603g2	bs9603h2	Clean. Increased airflow by putting woodstrip in 23 and blocking 113, 123, 133.	dd	0	N	Y
73	bs9603g1	bs9603h1	Clean. Increased airflow by putting woodstrip in 23 and blocking 113, 123, 133.	ee	0	N	Y
73	bs9603g2	bs9603h1	Clean. Increased airflow by putting	ee	0	N	Y

			woodstrip in 23 and blocking 113, 123, 133.				
73	bs9603g1	bs9603h2	Clean. Increased airflow by putting woodstrip in 23 and blocking 113, 123, 133.	ee	0	N	Y
73	bs9603g2	bs9603h2	Clean. Increased airflow by putting woodstrip in 23 and blocking 113, 123, 133.	ee	0	N	Y
13	bs9603g1	bs9603i1	blocked. Also blocked 83,93,103,113. Dif airflow.	ff	3	Y	Y
13	bs9603g2	bs9603i1	blocked. Also blocked 83,93,103,113. Dif airflow.	ff	3	Y	Y
23	bs9603g1	bs9603i1	Clean. Blocked 13, 83, 93, 103, 113. Dif airflow.	gg	0	N	Y
23	bs9603g2	bs9603i1	Clean. Blocked 13, 83, 93, 103, 113. Dif airflow.	gg	0	N	Y
33	bs9603g1	bs9603i1	Clean. Blocked 13, 83, 93, 103, 113. Dif airflow.	hh	0	N	Y
33	bs9603g2	bs9603i1	Clean. Blocked 13, 83, 93, 103, 113. Dif airflow.	hh	0	N	Y
43	bs9603g1	bs9603i1	Clean. Blocked 13, 83, 93, 103, 113. Dif airflow.	ii	0	N	Y
43	bs9603g2	bs9603i1	Clean. Blocked 13, 83, 93, 103, 113. Dif airflow.	ii	0	N	Y
53	bs9603g1	bs9603i1	Clean. Blocked 13, 83, 93, 103, 113. Dif airflow.	jj	0	N	Y
53	bs9603g2	bs9603i1	Clean. Blocked 13, 83, 93, 103, 113. Dif airflow.	jj	0	N	Y
63	bs9603g1	bs9603i1	Clean. Blocked 13, 83, 93, 103, 113. Dif airflow.	kk	0	N	Y
63	bs9603g2	bs9603i1	Clean. Blocked 13, 83, 93, 103, 113. Dif airflow.	kk	0	N	Y
73	bs9603g1	bs9603i1	Clean. Blocked 13, 83, 93, 103, 113. Dif airflow.	ll	0	N	Y
73	bs9603g2	bs9603i1	Clean. Blocked 13, 83, 93, 103, 113. Dif airflow.	ll	0	N	Y
83	bs9603b1	bs9603c1	103 and 113 blocked to increase airflow.	mm	0	N	Y
83	bs9603b2	bs9603c1	103 and 113 blocked to increase airflow.	mm	0	N	Y
83	bs9603b1	bs9603c2	133 blocked only with screen left infront of 103.	nn	0	N	Y
83	bs9603b2	bs9603c2	133 blocked only with screen left infront of 103.	nn	0	N	Y
93	bs9603b1	bs9603c1	103 and 113 blocked to increase airflow.	oo	0	N	Y
93	bs9603b2	bs9603c1	103 and 113 blocked to increase airflow.	oo	0	N	Y
93	bs9603b1	bs9603c2	133 blocked only with screen left infront of 103.	oo	0	N	Y
93	bs9603b2	bs9603c2	133 blocked only with screen left infront of 103.	oo	0	N	Y
13	bs9604b1	BS9604A1	Significant obstruction at hood opening.	pp	2	Y	Y
23	bs9604b1	BS9604A1	insignificant obstruction.	qq	0	N	Y
33	bs9604b1	BS9604A1	Insignificant settling.	rr	0	N	Y
43	bs9604b1	BS9604A1	Handful of clumps at the opening. blocked 25%.	ss	2	Y	Y
53	bs9604b1	BS9604A1	Few clumps removed from hood opening.	tt	1	Y	Y
63	bs9604b1	BS9604A1	<20% blocked.	uuu	1	Y	Y
73	bs9604b1	BS9604A1	SPH was not stable! 3 quarter sized chunks removed from hood opening	vvv	1	Y	Y

11	bd9603b1	bd9603a1	Repeat. 51, 71 cleaned, but 71 truth not known since clumps fell into tool.	uu	0	N	Y
11	bd9603b1	bd9603a2	Repeat. 51, 71 cleaned, but 71 truth not known since clumps fell into tool.	uu	0	N	Y
21	bd9603b1	bd9603a1	Repeat. 51, 71 cleaned, but 71 truth not known since clumps fell into tool.	vv	0	N	Y
21	bd9603b1	bd9603a2	Repeat. 51, 71 cleaned, but 71 truth not known since clumps fell into tool.	vv	0	N	Y
31	bd9603b1	bd9603a1	Repeat. 51, 71 cleaned, but 71 truth not known since clumps fell into tool.	ww	0	N	Y
31	bd9603b1	bd9603a2	Repeat. 51, 71 cleaned, but 71 truth not known since clumps fell into tool.	ww	0	N	Y
41	bd9603b1	bd9603a1	Repeat. 51, 71 cleaned, but 71 truth not known since clumps fell into tool.	xx	0	N	Y
41	bd9603b1	bd9603a2	Repeat. 51, 71 cleaned, but 71 truth not known since clumps fell into tool.	xx	0	N	Y
51	bd9603b1	bd9603a1	Substantial blockage removed upstream of SPH. See photos.	yy	2	Y	Y
51	bd9603b1	bd9603a2	Substantial blockage removed upstream of SPH. See photos.	yy	2	Y	Y
61	bd9603b1	bd9603a1		zz	0	N	Y
61	bd9603b1	bd9603a2		zz	0	N	Y
111	bd9603d1	bd9603c2	Repeat. Duct 141 cleanout out.	aaa	0	N	Y
111	bd9603d1	bd9603c3	Repeat. Duct 141 cleanout out.	aaa	0	N	Y
111	bd9603d2	bd9603c2	Repeat. Duct 141 cleanout out.	aaa	0	N	Y
111	bd9603d2	bd9603c3	Repeat. Duct 141 cleanout out.	aaa	0	N	Y
121	bd9603d1	bd9603c1	Repeat. Duct 141 cleanout out.	bbb	0	N	Y
121	bd9603d1	bd9603c2	Repeat. Duct 141 cleanout out.	bbb	0	N	Y
121	bd9603d1	bd9603c3	Repeat. Duct 141 cleanout out.	bbb	0	N	Y
121	bd9603d2	bd9603c1	Repeat. Duct 141 cleanout out.	bbb	0	N	Y
121	bd9603d2	bd9603c2	Repeat. Duct 141 cleanout out.	bbb	0	N	Y
121	bd9603d2	bd9603c3	Repeat. Duct 141 cleanout out.	bbb	0	N	Y
131	bd9603d1	bd9603c1	Repeat. Duct 141 cleanout out.	ccc	0	N	Y
131	bd9603d1	bd9603c2	Repeat. Duct 141 cleanout out.	ccc	0	N	Y
131	bd9603d1	bd9603c3	Repeat. Duct 141 cleanout out.	ccc	0	N	Y
131	bd9603d2	bd9603c1	Repeat. Duct 141 cleanout out.	ccc	0	N	Y
131	bd9603d2	bd9603c2	Repeat. Duct 141 cleanout out.	ccc	0	N	Y
131	bd9603d2	bd9603c3	Repeat. Duct 141 cleanout out.	ccc	0	N	Y
141	bd9603d1	bd9603c1	Big chunk upstream of SPH at back of tool. Also removed settling bet. H and End (1/10th full). See pics 7 - 10 and grey chunk on desk.	ddd	3	Y	Y
141	bd9603d1	bd9603c2	Big chunk upstream of SPH at back of tool. Also removed settling bet. H and End (1/10th full). See pics 7 - 10 and grey chunk on desk.	ddd	3	Y	Y
141	bd9603d1	bd9603c3	Big chunk upstream of SPH at back of tool. Also removed settling bet. H and End (1/10th full). See pics 7 - 10 and grey chunk on desk.	ddd	3	Y	Y
141	bd9603d2	bd9603c1	Big chunk upstream of SPH at back of tool. Also removed settling bet. H and End (1/10th full). See pics 7 - 10 and grey chunk on desk.	ddd	3	Y	Y
141	bd9603d2	bd9603c2	Big chunk upstream of SPH at back of tool. Also removed settling bet.	ddd	3	Y	Y

			H and End (1/10th full). See pics 7 - 10 and grey chunk on desk.				
141	bd9603d2	bd9603c3	Big chunk upstream of SPH at back of tool. Also removed settling bet. H and End (1/10th full). See pics 7 - 10 and grey chunk on desk.	ddd	3	Y	Y
151	bd9603d1	bd9603c1	Repeat. Duct 141 cleanout out.	eee	0	N	Y
151	bd9603d1	bd9603c2	Repeat. Duct 141 cleanout out.	eee	0	N	Y
151	bd9603d1	bd9603c3	Repeat. Duct 141 cleanout out.	eee	0	N	Y
151	bd9603d2	bd9603c1	Repeat. Duct 141 cleanout out.	eee	0	N	Y
151	bd9603d2	bd9603c2	Repeat. Duct 141 cleanout out.	eee	0	N	Y
151	bd9603d2	bd9603c3	Repeat. Duct 141 cleanout out.	eee	0	N	Y
131	bd9603d1	bd9603e1	Repeat. Increase airflow by blocking 111,121, 151.	fff	0	N	Y
131	bd9603d2	bd9603e1	Repeat. Increase airflow by blocking 111,121, 151.	fff	0	N	Y
11	bd9604a1	bd9604b1	Obstructions inserted in 31 and 71 bet H and mid/end.	ggg	0	N	Y
11	bd9604a2	bd9604b1	Obstructions inserted in 31 and 71 bet H and mid/end.	ggg	0	N	Y
21	bd9604a1	bd9604b1	Obstructions inserted in 31 and 71 bet H and mid/end.	hhh	0	N	Y
21	bd9604a2	bd9604b1	Obstructions inserted in 31 and 71 bet H and mid/end.	hhh	0	N	Y
31	bd9604a1	bd9604b1	Obstructions inserted in 31 and 71 bet H and mid/end.	iii	1	N	Y
31	bd9604a2	bd9604b1	Obstructions inserted in 31 and 71 bet H and mid/end.	iii	1	N	Y
41	bd9604a1	bd9604b1	Obstructions inserted in 31 and 71 bet H and mid/end.	jjj	0	N	Y
41	bd9604a2	bd9604b1	Obstructions inserted in 31 and 71 bet H and mid/end.	jjj	0	N	Y
51	bd9604a1	bd9604b1	Obstructions inserted in 31 and 71 bet H and mid/end.	kkk	0	N	Y
51	bd9604a2	bd9604b1	Obstructions inserted in 31 and 71 bet H and mid/end.	kkk	0	N	Y
61	bd9604a1	bd9604b1	Obstructions inserted in 31 and 71 bet H and mid/end.	lll	0	N	Y
61	bd9604a2	bd9604b1	Obstructions inserted in 31 and 71 bet H and mid/end.	lll	0	N	Y
71	bd9604a1	bd9604b1	Obstructions inserted in 31 and 71 bet H and mid/end.	mmm	1	N	Y
71	bd9604a2	bd9604b1	Obstructions inserted in 31 and 71 bet H and mid/end.	mmm	1	N	Y
11	bd9604a1	bd9604c1	Larger obstructions inserted in 31 and 71 bet H and mid/end.	nnn	0	N	Y
11	bd9604a2	bd9604c1	Larger obstructions inserted in 31 and 71 bet H and mid/end.	nnn	0	N	Y
21	bd9604a1	bd9604c1	Larger obstructions inserted in 31 and 71 bet H and mid/end.	ooo	0	N	Y
21	bd9604a2	bd9604c1	Larger obstructions inserted in 31 and 71 bet H and mid/end.	ooo	0	N	Y
31	bd9604a1	bd9604c1	Larger obstructions inserted in 31 and 71 bet H and mid/end.	ppp	2	N	Y
31	bd9604a2	bd9604c1	Larger obstructions inserted in 31 and 71 bet H and mid/end.	ppp	2	N	Y
41	bd9604a1	bd9604c1	Larger obstructions inserted in 31 and 71 bet H and mid/end.	qqq	0	N	Y
41	bd9604a2	bd9604c1	Larger obstructions inserted in 31 and 71 bet H and mid/end.	qqq	0	N	Y
51	bd9604a1	bd9604c1	Larger obstructions inserted in 31 and 71 bet H and mid/end.	rrr	0	N	Y
51	bd9604a2	bd9604c1	Larger obstructions inserted in 31 and 71 bet H and mid/end.	rrr	0	N	Y

61	bd9604a1	bd9604c1	Larger obstructions inserted in 31 and 71 bet H and mid/end.	sss	0	N	Y
61	bd9604a2	bd9604c1	Larger obstructions inserted in 31 and 71 bet H and mid/end.	sss	0	N	Y
71	bd9604a1	bd9604c1	Larger obstructions inserted in 31 and 71 bet H and mid/end.	ttt	3	N	Y
71	bd9604a2	bd9604c1	Larger obstructions inserted in 31 and 71 bet H and mid/end.	ttt	3	N	Y

Date	Filename	ID	Dia [in]	Tdb [C]	Twb [C]	*Vmeas*	*Qact*	SPH	SPen	SP ratio	Log trans'd SP ratio	VP_{avg}	Xend
3/19/96 10:00	bd960319	11	3	16	11.6	*3122.6*	*153.3*	1.64	3.76	0.436	-0.452	0.608	5.184
3/5/96 12:01	bd9603a1	11	3	14	9.5	*3213.7*	*157.8*	1.78	4.14	0.43	-0.444	0.644	5.429
3/5/96 12:45	bd9603a2	11	3	14	9.5	*3231.2*	*158.6*	1.8	4.05	0.444	-0.462	0.651	5.221
3/5/96 14:01	bd9603b1	11	3	15.7	10.3	*3362.1*	*165*	1.77	4.03	0.439	-0.455	0.702	4.741
4/5/96 12:43	bd9604a1	11	3	19.5	13	*2811.8*	*138*	1.4	3.26	0.429	-0.442	0.491	5.64
4/5/96 13:16	bd9604a2	11	3	19.5	13	*2859.9*	*140.4*	1.37	3.16	0.434	-0.449	0.51	5.196
4/5/96 14:00	bd9604b1	11	3	19.5	13	*2859.9*	*140.4*	1.37	3.19	0.429	-0.442	0.51	5.255
4/5/96 14:55	bd9604c1	11	3	19.5	13	*2904.4*	*142.6*	1.41	3.25	0.434	-0.449	0.526	5.179
2/13/96 13:30	bs9602a3	13	4	64.4	53.6	*2,577*	*224.86*	1.11	2	0.555	-0.621	0.414	3.831
2/13/96 15:30	bs9602b1	13	4	64.4	53.6	*2,383*	*207.93*	0.96	1.58	0.607	-0.705	0.354	3.463
2/13/96 16:15	bs9602b2	13	4	64.4	53.6	*2,406*	*209.98*	0.94	1.57	0.601	-0.695	0.361	3.349
3/19/96 12:13	bs960319	13	4	16	11.6	*2,254*	*196.67*	0.81	1.29	0.629	-0.743	0.317	3.069
3/21/96 9:29	bs9603g1	13	4	16.5	10.5	*2,201*	*192.05*	0.79	1.29	0.61	-0.71	0.302	3.272
3/21/96 10:52	bs9603g2	13	4	16.5	10.5	*2,223*	*193.95*	0.76	1.26	0.605	-0.702	0.308	3.091
3/21/96 12:39	bs9603h1	13	4	14.5	9.3	*2,449*	*213.72*	0.94	1.55	0.608	-0.707	0.374	3.144
3/21/96 13:50	bs9603h2	13	4	14.5	9.3	*2,472*	*215.71*	0.93	1.53	0.606	-0.703	0.381	3.016
3/21/96 15:10	bs9603i1	13	4	14.5	9.3	*1,352*	*118.00*	2.7	2.84	0.951	-1.573	0.114	23.91
3/19/96 10:00	bd960319	21	4	16	11.6	*3423.9*	*298.8*	1.28	4.11	0.311	-0.3	0.731	4.622
3/5/96 12:01	bd9603a1	21	4	14	9.5	*3516.4*	*306.9*	1.4	4.5	0.311	-0.3	0.771	4.837
3/5/96 12:45	bd9603a2	21	4	14	9.5	*3635.2*	*317.2*	1.34	4.4	0.305	-0.293	0.824	4.34
3/5/96 14:01	bd9603b1	21	4	15.7	10.3	*3398.1*	*296.5*	0.97	4.32	0.225	-0.208	0.72	5
4/5/96 12:43	bd9604a1	21	4	19.5	13	*3248.5*	*283.5*	1.22	3.53	0.346	-0.34	0.658	4.365
4/5/96 13:16	bd9604a2	21	4	19.5	13	*3287.7*	*286.9*	1.21	3.5	0.346	-0.34	0.674	4.193
4/5/96 14:00	bd9604b1	21	4	19.5	13	*3208.7*	*280*	1.14	3.47	0.329	-0.32	0.642	4.405
4/5/96 14:55	bd9604c1	21	4	19.5	13	*3360.1*	*293.2*	1.15	3.55	0.324	-0.315	0.704	4.043

Date	Filename	ID	Dia [in]	Tdb [C]	Twb [C]	*Vmeas*	*Qact*	SPH	SPen	SP ratio	Log trans'd SP ratio	VP_{avg}	Xend
2/13/96 11:00	bs9602a1	23	3	64.4	53.6	*2,478*	*121.66*	1.33	1.97	0.675	-0.827	0.383	4.144
2/13/96 12:30	bs9602a2	23	3	64.4	53.6	*2,446*	*120.06*	1.25	1.95	0.641	-0.764	0.373	4.228
2/13/96 15:30	bs9602b1	23	3	64.4	53.6	*2,197*	*107.85*	1	1.47	0.68	-0.836	0.301	3.884
2/13/96 16:15	bs9602b2	23	3	64.4	53.6	*2,130*	*104.58*	1	1.48	0.676	-0.829	0.283	4.23
3/19/96 12:13	bs960319	23	3	16	11.6	*1,933*	*94.89*	0.85	1.23	0.689	-0.854	0.233	4.279
3/21/96 9:29	bs9603g1	23	3	16.5	10.5	*1,954*	*95.90*	0.85	1.21	0.7	-0.875	0.238	4.084
3/21/96 10:52	bs9603g2	23	3	16.5	10.5	*1,912*	*93.87*	0.82	1.16	0.703	-0.881	0.228	4.088
3/21/96 12:39	bs9603h1	23	3	14.5	9.3	*1,887*	*92.62*	0.94	1.46	0.64	-0.762	0.222	5.577
3/21/96 13:50	bs9603h2	23	3	14.5	9.3	*1,883*	*92.41*	1.08	1.43	0.755	-0.992	0.221	5.471
3/21/96 15:10	bs9603i1	23	3	14.5	9.3	*3,068*	*150.61*	1.95	2.78	0.701	-0.877	0.587	3.736
3/19/96 10:00	bd960319	31	3	16	11.6	*3882.7*	*190.6*	2.02	3.68	0.549	-0.612	0.94	2.915
3/5/96 12:01	bd9603a1	31	3	14	9.5	*4072.2*	*199.9*	2.15	4.05	0.531	-0.584	1.034	2.917
3/5/96 12:45	bd9603a2	31	3	14	9.5	*4123.1*	*202.4*	2.15	3.97	0.542	-0.601	1.06	2.745
3/5/96 14:01	bd9603b1	31	3	15.7	10.3	*3990.6*	*195.9*	2.14	3.93	0.545	-0.605	0.993	2.958
4/5/96 12:43	bd9604a1	31	3	19.5	13	*3657.2*	*179.5*	1.69	3.16	0.535	-0.59	0.834	2.789
4/5/96 13:16	bd9604a2	31	3	19.5	13	*3657.2*	*179.5*	1.69	3.13	0.54	-0.598	0.834	2.753
4/5/96 14:00	bd9604b1	31	3	19.5	13	*3488.9*	*171.3*	1.62	3.13	0.518	-0.565	0.759	3.124
4/5/96 14:55	bd9604c1	31	3	19.5	13	*3326.5*	*163.3*	1.46	3.21	0.455	-0.477	0.69	3.652
2/13/96 11:00	bs9602a1	33	3	64.4	53.6	*633*	*31.08*	0.11	2.43	0.046	-0.039	0.025	96.2
2/13/96 12:30	bs9602a2	33	3	64.4	53.6	*620*	*30.45*	0.11	2.48	0.045	-0.038	0.024	102.3
2/13/96 15:30	bs9602b1	33	3	64.4	53.6	*2,096*	*102.90*	1.04	1.32	0.788	-1.069	0.274	3.818
2/13/96 16:15	bs9602b2	33	3	64.4	53.6	*2,406*	*118.11*	1.04	1.29	0.806	-1.114	0.361	2.573
3/19/96 12:13	bs960319	33	3	16	11.6	*2,018*	*99.07*	0.88	1.11	0.795	-1.086	0.254	3.37
3/21/96 9:29	bs9603g1	33	3	16.5	10.5	*1,945*	*95.50*	0.87	1.09	0.799	-1.096	0.236	3.619
3/21/96 10:52	bs9603g2	33	3	16.5	10.5	*1,883*	*92.41*	0.85	1.06	0.803	-1.106	0.221	3.796
3/21/96 12:39	bs9603h1	33	3	14.5	9.3	*2,208*	*108.39*	1.01	1.27	0.795	-1.086	0.304	3.178
3/21/96 13:50	bs9603h2	33	3	14.5	9.3	*2,190*	*107.49*	1.02	1.28	0.797	-1.091	0.299	3.281
3/21/96 15:10	bs9603i1	33	3	14.5	9.3	*2,740*	*134.48*	1.64	2.02	0.812	-1.129	0.468	3.316
3/19/96 10:00	bd960319	41	3	16	11.6	*3733.2*	*183.3*	3.05	4.15	0.735	-0.948	0.869	3.776

Date	Filename	ID	Dia [in]	Tdb [C]	Twb [C]	*Vmeas*	*Qact*	SPH	SPen	SP ratio	Log trans'd SP ratio	VP_{avg}	Xend
3/5/96 12:01	bd9603a1	41	3	14	9.5	*3790.7*	*186.1*	3.48	4.74	0.734	-0.946	0.896	4.29
3/5/96 12:45	bd9603a2	41	3	14	9.5	*3984.6*	*195.6*	3.51	4.54	0.773	-1.033	0.99	3.586
3/5/96 14:01	bd9603b1	41	3	15.7	10.3	*3799.2*	*186.5*	3.4	4.44	0.766	-1.017	0.9	3.933
4/5/96 12:43	bd9604a1	41	3	19.5	13	*3500.4*	*171.8*	2.61	3.52	0.741	-0.961	0.794	3.607
4/5/96 13:16	bd9604a2	41	3	19.5	13	*3482*	*170.9*	2.58	3.54	0.729	-0.935	0.76	3.683
4/5/96 14:00	bd9604b1	41	3	19.5	13	*3423.9*	*168.1*	2.57	3.51	0.732	-0.942	0.759	3.802
4/5/96 14:55	bd9604c1	41	3	19.5	13	*3507.2*	*172.2*	2.63	3.52	0.747	-0.974	0.774	3.589
2/13/96 11:00	bs9602a1	43	3	64.4	53.6	*1,535*	*75.37*	0.11	2.36	0.047	-0.04	0.147	15.05
2/13/96 12:30	bs9602a2	43	3	64.4	53.6	*1,215*	*59.63*	2.28	2.39	0.954	-1.585	0.092	24.98
2/13/96 13:30	bs9602a3	43	3	64.4	53.6	*1,449*	*71.15*	2.28	2.38	0.958	-1.601	0.131	17.17
2/13/96 15:30	bs9602b1	43	3	64.4	53.6	*2,119*	*104.02*	1.04	1.36	0.765	-1.015	0.28	3.857
2/13/96 16:15	bs9602b2	43	3	64.4	53.6	*1,891*	*92.83*	1.05	1.36	0.772	-1.031	0.223	5.099
3/19/96 12:13	bs960319	43	3	16	11.6	*2,002*	*98.29*	0.92	1.16	0.789	-1.071	0.25	3.64
3/21/96 9:29	bs9603g1	43	3	16.5	10.5	*1,994*	*97.90*	0.9	1.12	0.803	-1.106	0.248	3.516
3/21/96 10:52	bs9603g2	43	3	16.5	10.5	*2,081*	*102.15*	0.89	1.15	0.771	-1.029	0.27	3.259
3/21/96 12:39	bs9603h1	43	3	14.5	9.3	*2,240*	*109.98*	1.04	1.34	0.776	-1.04	0.313	3.281
3/21/96 13:50	bs9603h2	43	3	14.5	9.3	*2,186*	*107.31*	1.04	1.34	0.776	-1.04	0.298	3.497
3/21/96 15:10	bs9603i1	43	3	14.5	9.3	*2,751*	*135.05*	1.67	2.11	0.791	-1.076	0.472	3.47
3/19/96 10:00	bd960319	51	4	16	11.6	*4313.2*	*376.4*	3.25	4.08	0.797	-1.091	1.118	2.517
3/5/96 12:01	bd9603a1	51	4	14	9.5	*3248.5*	*283.5*	2.93	4.25	0.689	-0.854	0.658	5.459
3/5/96 12:45	bd9603a2	51	4	14	9.5	*3233.6*	*282.2*	2.88	4.21	0.684	-0.844	0.652	5.457
3/5/96 14:01	bd9603b1	51	4	15.7	10.3	*4022.7*	*351*	3.23	4.09	0.79	-1.074	1.009	3.054
4/5/96 12:43	bd9604a1	51	4	19.5	13	*3683.4*	*321.4*	2.3	2.99	0.769	-1.024	0.781	2.534
4/5/96 13:16	bd9604a2	51	4	19.5	13	*3637.4*	*317.4*	2.29	2.98	0.768	-1.022	0.794	2.612
4/5/96 14:00	bd9604b1	51	4	19.5	13	*3628.6*	*316.7*	2.29	2.97	0.771	-1.029	0.765	2.618
4/5/96 14:55	bd9604c1	51	4	19.5	13	*3703*	*323.1*	2.34	3.04	0.77	-1.026	0.785	2.556
2/13/96 11:00	bs9602a1	53	3	64.4	53.6	*2,710*	*133.04*	1.66	2.21	0.751	-0.983	0.458	3.825

Date	Filename	ID	Dia [in]	Tdb [C]	Twb [C]	*Vmeas*	*Qact*	SPH	SPen	SP ratio	Log trans'd SP ratio	VP_{avg}	Xend
2/13/96 12:30	bs9602a2	53	3	64.4	53.6	*2,772*	*136.05*	1.65	2.21	0.747	-0.974	0.479	3.614
2/13/96 15:30	bs9602b1	53	3	64.4	53.6	*2,182*	*107.13*	1.14	1.49	0.765	-1.015	0.297	4.017
2/13/96 16:15	bs9602b2	53	3	64.4	53.6	*1,791*	*87.91*	1.19	1.48	0.804	-1.109	0.2	6.4
3/19/96 12:13	bs960319	53	3	16	11.6	*3,130*	*153.66*	0.97	1.24	0.78	-1.05	0.611	1.029
3/21/96 9:29	bs9603g1	53	3	16.5	10.5	*2,123*	*104.21*	0.89	1.22	0.727	-0.931	0.281	3.342
3/21/96 10:52	bs9603g2	53	3	16.5	10.5	*2,197*	*107.85*	0.87	1.22	0.711	-0.898	0.301	3.053
3/21/96 12:39	bs9603h1	53	3	14.5	9.3	*2,349*	*115.30*	1.06	1.43	0.741	-0.961	0.344	3.157
3/21/96 13:50	bs9603h2	53	3	14.5	9.3	*2,258*	*110.85*	1.08	1.42	0.761	-1.006	0.318	3.465
3/21/96 15:10	bs9603i1	53	3	14.5	9.3	*2,891*	*141.89*	1.6	2.2	0.727	-0.931	0.521	3.223
3/19/96 10:00	bd960319	61	4	16	11.6	*759.83*	*66.31*	4.22	3.54	1.192	-5.011	0.03	97.33
3/5/96 12:01	bd9603a1	61	4	14	9.5	*1139.8*	*99.46*	4.09	3.8	1.076	-2.27	0.081	45.91
3/5/96 12:45	bd9603a2	61	4	14	9.5	*1125.6*	*98.23*	4.02	3.82	1.052	-2.093	0.079	47.35
3/5/96 14:01	bd9603b1	61	4	15.7	10.3	*1310*	*114.3*	3.8	3.55	1.07	-2.223	0.105	32.18
4/5/96 12:43	bd9604a1	61	4	19.5	13	*1941.3*	*169.4*	2.47	2.46	1.004	-1.812	0.224	9.468
4/5/96 13:16	bd9604a2	61	4	19.5	13	*1891.1*	*165*	2.48	2.51	0.988	-1.733	0.208	10.26
4/5/96 14:00	bd9604b1	61	4	19.5	13	*1865.5*	*162.8*	2.56	2.55	1.004	-1.812	0.212	10.75
4/5/96 14:55	bd9604c1	61	4	19.5	13	*1937.2*	*169.1*	2.57	2.56	1.004	-1.812	0.224	9.94
2/13/96 11:00	bs9602a1	63	3	64.4	53.6	*1,334*	*65.49*	2.09	2.19	0.954	-1.585	0.111	18.73
2/13/96 12:30	bs9602a2	63	3	64.4	53.6	*1,334*	*65.49*	2.11	2.24	0.942	-1.537	0.111	19.18
2/13/96 15:30	bs9602b1	63	3	64.4	53.6	*2,495*	*122.45*	0.93	1.52	0.613	-0.715	0.388	2.918
2/13/96 16:15	bs9602b2	63	3	64.4	53.6	*2,251*	*110.50*	0.91	1.54	0.592	-0.68	0.316	3.873
3/19/96 12:13	bs960319	63	3	16	11.6	*1,978*	*97.10*	0.8	1.23	0.65	-0.78	0.244	4.041
3/21/96 9:29	bs9603g1	63	3	16.5	10.5	*2,022*	*99.27*	0.78	1.2	0.649	-0.778	0.255	3.706
3/21/96 10:52	bs9603g2	63	3	16.5	10.5	*2,034*	*99.85*	0.81	1.22	0.661	-0.8	0.258	3.729
3/21/96 12:39	bs9603h1	63	3	14.5	9.3	*2,297*	*112.75*	0.96	1.42	0.678	-0.832	0.329	3.316
3/21/96 13:50	bs9603h2	63	3	14.5	9.3	*2,127*	*104.39*	0.89	1.42	0.627	-0.739	0.282	4.035
3/21/96 15:10	bs9603i1	63	3	14.5	9.3	*2,716*	*133.33*	1.39	2.19	0.635	-0.753	0.46	3.761

Date	Filename	ID	Dia [in]	Tdb [C]	Twb [C]	*Vmeas*	*Qact*	SPH	SPen	SP ratio	Log trans'd SP ratio	VP_{avg}	Xend
3/19/96 10:00	bd960319	71	3	16	11.6	*877.38*	*43.07*	3.46	3.54	0.977	-1.683	0.046	72.75
4/5/96 12:43	bd9604a1	71	3	19.5	13	*1449.5*	*71.15*	2.71	2.87	0.944	-1.545	0.13	20.91
4/5/96 13:16	bd9604a2	71	3	19.5	13	*1410.2*	*69.22*	2.7	2.86	0.944	-1.545	0.116	22.06
4/5/96 14:00	bd9604b1	71	3	19.5	13	*1381.5*	*67.81*	2.66	2.84	0.937	-1.518	0.112	22.87
4/5/96 14:55	bd9604c1	71	3	19.5	13	*1358.1*	*66.66*	2.44	2.93	0.833	-1.185	0.109	24.48
2/13/96 11:00	bs9602a1	73	3	64.4	53.6	*2,265*	*111.20*	1.91	3.05	0.626	-0.737	0.32	8.531
2/13/96 12:30	bs9602a2	73	3	64.4	53.6	*2,215*	*108.74*	1.87	3.02	0.619	-0.725	0.306	8.869
2/13/96 15:30	bs9602b1	73	3	64.4	53.6	*2,389*	*117.29*	1.3	2.55	0.51	-0.553	0.356	6.163
2/13/96 16:15	bs9602b2	73	3	64.4	53.6	*2,352*	*115.46*	1.32	2.56	0.516	-0.562	0.345	6.42
3/19/96 12:13	bs960319	73	3	16	11.6	*2,233*	*109.63*	1.07	2.11	0.507	-0.549	0.311	5.785
3/21/96 9:29	bs9603g1	73	3	16.5	10.5	*2,204*	*108.21*	1	2.08	0.48	-0.511	0.303	5.865
3/21/96 10:52	bs9603g2	73	3	16.5	10.5	*2,301*	*112.93*	1.02	2.12	0.481	-0.512	0.33	5.424
3/21/96 12:39	bs9603h1	73	3	14.5	9.3	*2,416*	*118.60*	1.16	2.44	0.475	-0.504	0.364	5.703
3/21/96 13:50	bs9603h2	73	3	14.5	9.3	*2,423*	*118.93*	1.16	2.43	0.477	-0.507	0.366	5.639
3/21/96 15:10	bs9603i1	73	3	14.5	9.3	*3,042*	*149.32*	1.8	3.73	0.483	-0.515	0.577	5.464
3/19/96 10:00	bd960319	81	3	16	11.6	*4140.5*	*203.2*	1.91	2.88	0.663	-0.804	1.069	1.694
2/15/96 10:00	bs9602c1	83	3	58.1	49.1	*2,396*	*117.62*	0.7	1.34	0.521	-0.569	0.358	2.743
3/19/96 12:13	bs960319	83	3	16	11.6	*1,795*	*88.13*	0.38	0.686	0.555	-0.621	0.201	2.413
3/7/96 10:40	bs9603a1	83	3	16.8	11.8	*1,925*	*94.48*	0.46	0.867	0.532	-0.586	0.231	2.753
3/7/96 12:00	bs9603a2	83	3	15.5	11.2	*1,958*	*96.10*	0.43	0.827	0.519	-0.567	0.239	2.46
3/7/96 13:30	bs9603b1	83	3	15.5	11.2	*1,777*	*87.25*	0.41	0.762	0.531	-0.584	0.197	2.868
3/7/96 14:40	bs9603b2	83	3	15.5	11.2	*1,736*	*85.23*	0.42	0.791	0.527	-0.578	0.188	3.207
3/7/96 15:20	bs9603c1	83	3	15.5	11.2	*2,294*	*112.58*	0.63	1.18	0.537	-0.593	0.328	2.598
3/7/96 16:00	bs9603c2	83	3	15.5	6.29	*2,092*	*102.71*	0.51	0.987	0.521	-0.569	0.273	2.615
3/19/96 15:00	bs9603f1	83	3	16	11.6	*1,690*	*82.94*	0.37	0.694	0.532	-0.586	0.178	2.899
2/15/96 10:00	bs9602c1	93	3	58.1	49.1	*821*	*40.29*	1.27	1.27	1	-1.792	0.042	29.24
3/19/96 12:13	bs960319	93	3	16	11.6	*1,791*	*87.91*	0.47	0.63	0.744	-0.968	0.2	2.15

Date	Filename	ID	Dia [in]	Tdb [C]	Twb [C]	*Vmeas*	*Qact*	SPH	SPen	SP ratio	Log trans'd SP ratio	VP_{avg}	Xend
3/7/96 12:00	bs9603a2	93	3	15.5	11.2	*2,030*	*99.66*	0.6	0.754	0.793	-1.081	0.257	1.934
3/7/96 12:45	bs9603a3	93	3	15.5	11.2	*1,921*	*94.28*	0.56	0.738	0.762	-1.008	0.23	2.209
3/7/96 13:30	bs9603b1	93	3	15.5	11.2	*1,861*	*91.36*	0.59	0.718	0.827	-1.168	0.216	2.324
3/7/96 14:40	bs9603b2	93	3	15.5	11.2	*1,929*	*94.69*	0.6	0.738	0.816	-1.139	0.232	2.181
3/7/96 15:20	bs9603c1	93	3	15.5	11.2	*2,345*	*115.13*	0.93	1.09	0.854	-1.244	0.343	2.178
3/7/96 16:00	bs9603c2	93	3	15.5	11.2	*2,142*	*105.13*	0.74	0.907	0.814	-1.134	0.286	2.171
3/19/96 15:00	bs9603f1	93	3	16	11.6	*1,831*	*89.87*	0.47	0.63	0.751	-0.983	0.209	2.014
2/15/96 10:00	bs9602c1	103	4	58.1	49.1	*2,301*	*200.76*	1.18	1.8	0.656	-0.791	0.33	4.455
3/19/96 12:13	bs960319	103	4	16	11.6	*2,062*	*179.90*	1	1.45	0.686	-0.848	0.265	4.472
3/7/96 10:40	bs9603a1	103	4	16.8	11.8	*2,265*	*197.69*	1.24	1.8	0.689	-0.854	0.32	4.625
3/7/96 12:00	bs9603a2	103	4	15.5	11.2	*2,186*	*190.78*	1.21	1.74	0.695	-0.866	0.298	4.839
3/7/96 13:30	bs9603b1	103	4	15.5	11.2	*2,164*	*188.85*	1.16	1.68	0.69	-0.856	0.292	4.753
3/7/96 14:40	bs9603b2	103	4	15.5	11.2	*2,160*	*188.52*	1.14	1.67	0.683	-0.842	0.291	4.739
3/19/96 15:00	bs9603f1	103	4	16	11.6	*2,022*	*176.48*	1.01	1.48	0.682	-0.84	0.255	4.804
3/19/96 10:00	bd960319	111	3	16	11.6	*3644*	*178.9*	2.03	3.97	0.511	-0.555	0.847	3.795
3/13/96 12:00	bd9603c2	111	3	16.7	11.1	*3911.5*	*192*	2.15	4.39	0.49	-0.525	1.005	3.602
3/13/96 12:37	bd9603c3	111	3	16.7	11.1	*3888.9*	*190.9*	2.16	4.38	0.493	-0.529	0.994	3.645
3/13/96 15:00	bd9603d1	111	3	16.7	11.1	*3741.8*	*183.7*	1.96	4.05	0.484	-0.516	0.901	3.639
3/13/96 15:35	bd9603d2	111	3	16.7	11.1	*3703*	*181.8*	2	4.02	0.498	-0.536	0.895	3.702
2/15/96 10:00	bs9602c1	113	3	58.1	49.1	*2,809*	*137.89*	0.95	1.6	0.592	-0.68	0.492	2.252
3/19/96 12:13	bs960319	113	3	16	11.6	*2,602*	*127.70*	0.85	1.29	0.66	-0.799	0.422	2.057
3/7/96 10:40	bs9603a1	113	3	16.8	11.8	*2,915*	*143.11*	1.08	1.63	0.663	-0.804	0.53	2.075
3/7/96 12:00	bs9603a2	113	3	15.5	11.2	*2,967*	*145.65*	1.07	1.6	0.669	-0.815	0.549	1.914
3/7/96 13:30	bs9603b1	113	3	15.5	11.2	*2,731*	*134.05*	0.97	1.47	0.661	-0.8	0.465	2.161
3/7/96 14:40	bs9603b2	113	3	15.5	11.2	*2,843*	*139.56*	0.98	1.47	0.663	-0.804	0.504	1.917
3/19/96 15:00	bs9603f1	113	3	16	11.6	*2,656*	*130.40*	0.84	1.32	0.639	-0.76	0.44	2
3/19/96 10:00	bd960319	121	3	16	11.6	*2409.5*	*118.3*	1.45	3.17	0.457	-0.479	0.356	7.757

Date	Filename	ID	Dia [in]	Tdb [C]	Twb [C]	*Vmeas*	*Qact*	SPH	SPen	SP ratio	Log trans'd SP ratio	VP_{avg}	Xend
3/13/96 10:01	bd9603c1	121	3	16.7	11.1	*2567.4*	*126*	1.58	3.51	0.45	-0.47	0.392	7.54
3/13/96 12:00	bd9603c2	121	3	16.7	11.1	*2586*	*126.9*	1.54	3.41	0.452	-0.473	0.406	7.177
3/13/96 12:37	bd9603c3	121	3	16.7	11.1	*2548.6*	*125.1*	1.54	3.42	0.45	-0.47	0.387	7.444
3/13/96 15:00	bd9603d1	121	3	16.7	11.1	*2449.1*	*120.2*	1.41	3.13	0.45	-0.47	0.349	7.369
3/13/96 15:35	bd9603d2	121	3	16.7	11.1	*2416.1*	*118.6*	1.44	3.13	0.46	-0.483	0.347	7.599
2/15/96 10:00	bs9602c1	123	3	58.1	49.1	*760*	*37.30*	1.54	1.56	0.987	-1.729	0.036	42.33
3/19/96 12:13	bs960319	123	3	16	11.6	*811*	*39.80*	1.22	1.26	0.968	-1.643	0.041	29.73
3/7/96 10:40	bs9603a1	123	3	16.8	11.8	*670*	*32.89*	1.58	1.6	0.988	-1.733	0.028	56.14
3/7/96 12:00	bs9603a2	123	3	15.5	11.2	*670*	*32.89*	1.56	1.56	1	-1.792	0.028	54.71
3/7/96 13:30	bs9603b1	123	3	15.5	11.2	*922*	*45.26*	1.4	1.45	0.966	-1.635	0.053	26.36
3/7/96 14:40	bs9603b2	123	3	15.5	11.2	*877*	*43.07*	1.38	1.43	0.965	-1.63	0.048	28.79
3/19/96 15:00	bs9603f1	123	3	16	11.6	*840*	*41.23*	1.26	1.28	0.984	-1.715	0.044	28.09
3/19/96 10:00	bd960319	131	3	16	11.6	*2748.4*	*134.9*	2.07	2.6	0.796	-1.089	0.456	4.52
3/13/96 10:01	bd9603c1	131	3	16.7	11.1	*3255.9*	*159.8*	2.77	3.44	0.805	-1.111	0.634	4.204
3/13/96 12:00	bd9603c2	131	3	16.7	11.1	*3198.7*	*157*	2.75	3.46	0.795	-1.086	0.613	4.423
3/13/96 12:37	bd9603c3	131	3	16.7	11.1	*3196.2*	*156.9*	2.75	3.39	0.811	-1.126	0.6	4.322
3/13/96 15:00	bd9603d1	131	3	16.7	11.1	*2765.8*	*135.8*	2.03	2.55	0.796	-1.089	0.457	4.346
3/13/96 15:35	bd9603d2	131	3	16.7	11.1	*2765.8*	*135.8*	2.05	2.54	0.807	-1.116	0.459	4.325
3/13/96 15:59	bd9603e1	131	3	16.7	11.1	*3866.1*	*189.8*	4.04	5.04	0.802	-1.104	0.87	4.408
2/15/96 10:00	bs9602c1	133	3	58.1	49.1	*1,520*	*74.60*	1.95	2.18	0.894	-1.366	0.144	14.14
3/19/96 12:13	bs960319	133	3	16	11.6	*1,399*	*68.66*	1.65	1.84	0.897	-1.376	0.122	14.08
3/19/96 10:00	bd960319	141	3	16	11.6	*3102*	*152.3*	1.95	2.67	0.73	-0.937	0.596	3.45
3/13/96 10:01	bd9603c1	141	3	16.7	11.1	*1028.8*	*50.5*	3.32	3.38	0.982	-1.706	0.068	50.21
3/13/96 12:00	bd9603c2	141	3	16.7	11.1	*1021*	*50.12*	3.29	3.31	0.994	-1.762	0.065	49.92
3/13/96 12:37	bd9603c3	141	3	16.7	11.1	*1028.8*	*50.5*	3.28	3.33	0.985	-1.719	0.065	49.45
3/13/96 15:00	bd9603d1	141	3	16.7	11.1	*3171*	*155.7*	1.91	2.66	0.718	-0.912	0.633	3.242
3/13/96 15:35	bd9603d2	141	3	16.7	11.1	*3122.6*	*153.3*	1.9	2.64	0.72	-0.916	0.618	3.342

Date	Filename	ID	Dia [in]	Tdb [C]	Twb [C]	*Vmeas*	*Qact*	SPH	SPen	SP ratio	Log trans'd SP ratio	VP_{avg}	Xend
3/19/96 10:00	bd960319	151	3	16	11.6	*3117.5*	*153*	1.76	3.71	0.474	-0.503	0.626	5.122
3/13/96 10:01	bd9603c1	151	3	16.7	11.1	*3255.9*	*159.8*	1.98	4.07	0.486	-0.519	0.668	5.157
3/13/96 12:00	bd9603c2	151	3	16.7	11.1	*3362.5*	*165.1*	1.93	4.02	0.48	-0.511	0.725	4.702
3/13/96 12:37	bd9603c3	151	3	16.7	11.1	*3280.4*	*161*	1.9	3.95	0.481	-0.512	0.701	4.887
3/13/96 15:00	bd9603d1	151	3	16.7	11.1	*3153.3*	*154.8*	1.81	3.73	0.485	-0.518	0.649	5.016
3/13/96 15:35	bd9603d2	151	3	16.7	11.1	*3183.7*	*156.3*	1.78	3.73	0.477	-0.507	0.654	4.902
3/19/96 10:00	bd960319	161	3	16	11.6	*670.11*	*32.89*	3.75	3.74	1.003	-1.807	0	132.6